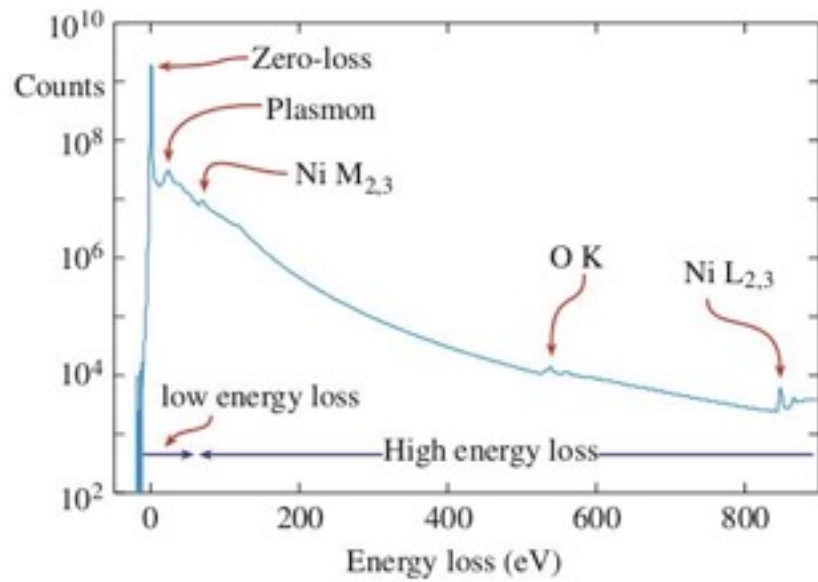
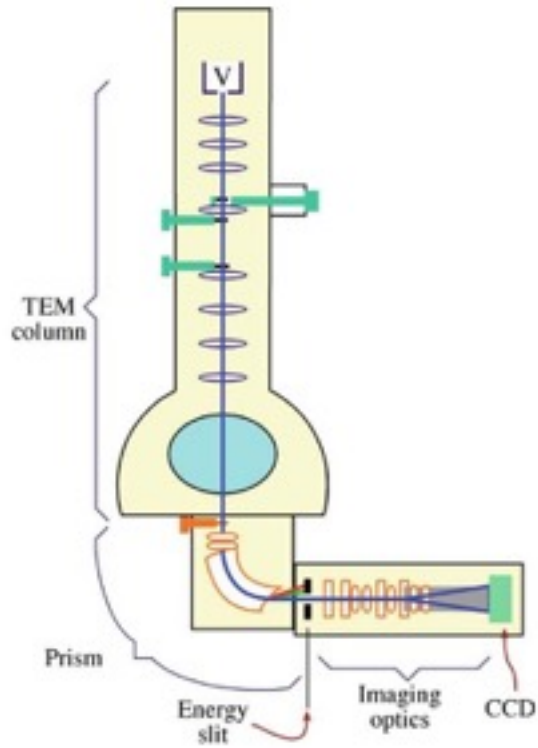


Electron Energy-Loss Spectrometry

Walid Hetaba
28.10.2016



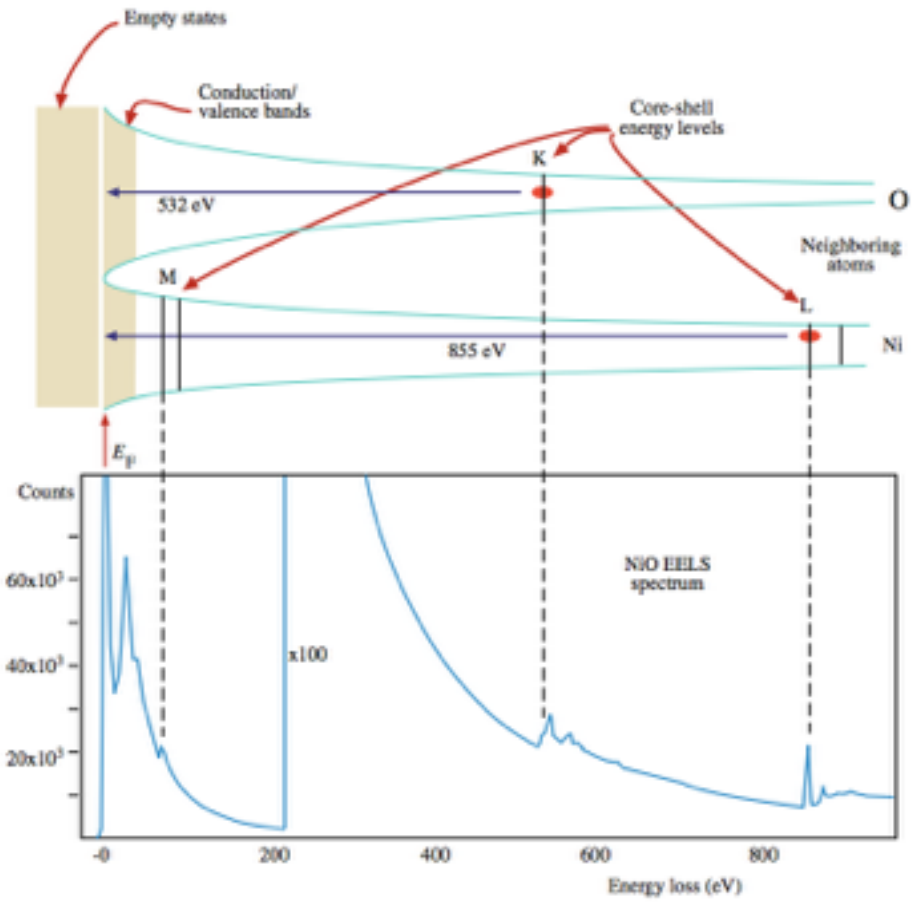
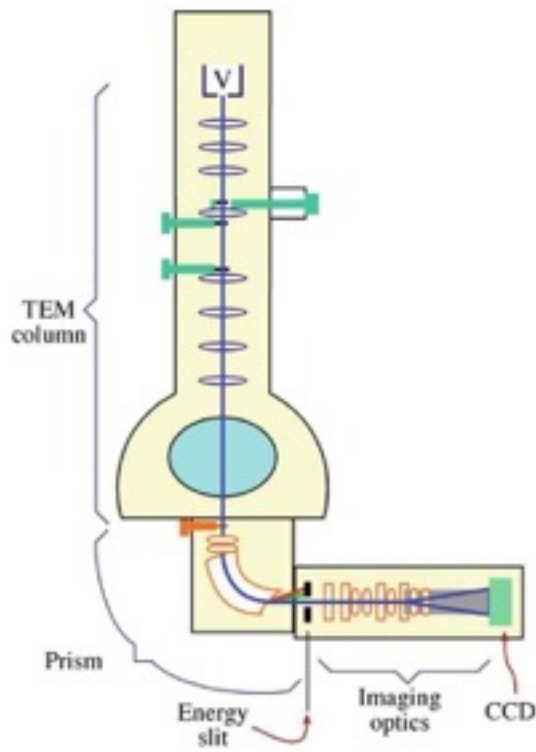
Energy loss spectrum



Williams, Carter: Transmission Electron Microscopy, Springer 2009



Energy loss spectrum

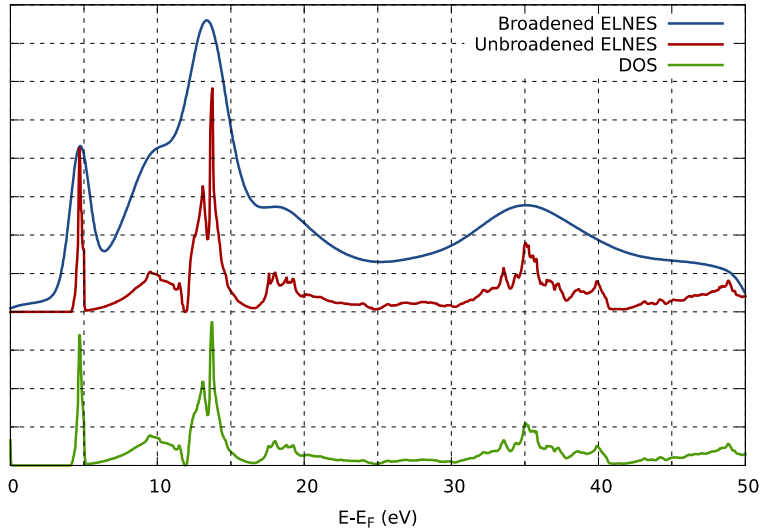


Williams, Carter: Transmission Electron Microscopy, Springer 2009

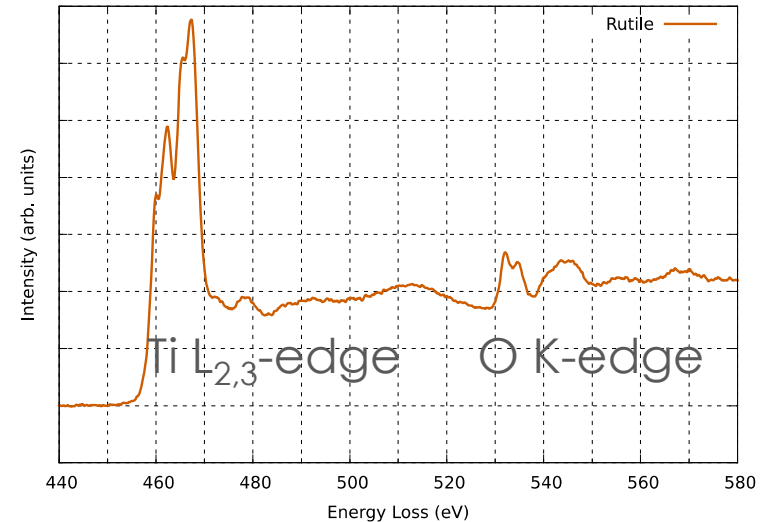


Energy loss near edge spectrum

ELNES



NiO, WIEN2k



TiO_2 , exp.

Hetaba et al., PRB 85 (2012), 205108



Formalism

Schrödinger equation:

$$\begin{aligned}\hat{H}\Psi(t) &= i\hbar \frac{\partial}{\partial t} \Psi(t) \\ \hat{H}\Psi &= E\Psi \\ \hat{H} &= -\frac{\hbar^2}{2m} \Delta + V(\mathbf{r}, t)\end{aligned}$$

Bra-Ket formalism:

$$|\Psi\rangle, \langle\Psi|, \langle\Psi|\Phi\rangle$$

$$\langle x|\Psi\rangle = \Psi(x)$$

$$\langle\Psi|x\rangle = \Psi^*(x)$$

$$\langle\Psi|\Psi\rangle = \int \Psi^*(x)\Psi(x)d^3x$$



Double differential scattering cross-section

$$W_{i \rightarrow f} = \frac{2\pi}{\hbar} \left| \left\langle \Psi_f \left| \hat{V} \right| \Psi_i \right\rangle \right|^2 d\nu_f \cdot \delta(E_{|f\rangle} - E_{|i\rangle})$$



Double differential scattering cross-section

$$W_{i \rightarrow f} = \frac{2\pi}{\hbar} \left| \left\langle \Psi_f \right| \hat{V} \left| \Psi_i \right\rangle \right|^2 d\nu_f \cdot \delta(E_{|f\rangle} - E_{|i\rangle})$$

$$\left| \Psi_{i,f} \right\rangle = \left| \psi_{i,f} \right\rangle \otimes \left| i,f \right\rangle \quad \left\langle \mathbf{r} \right| \psi_{i,f} \rangle = \left\langle \mathbf{r} \right| \mathbf{k}_{i,f} \rangle = \frac{1}{(2\pi)^{3/2}} e^{i \mathbf{k}_{i,f} \cdot \mathbf{r}}$$



Double differential scattering cross-section

$$W_{i \rightarrow f} = \frac{2\pi}{\hbar} \left| \left\langle \Psi_f \right| \hat{V} \left| \Psi_i \right\rangle \right|^2 d\nu_f \cdot \delta(E_{|f\rangle} - E_{|i\rangle})$$

$$\left| \Psi_{i,f} \right\rangle = \left| \psi_{i,f} \right\rangle \otimes \left| i,f \right\rangle \quad \left\langle \mathbf{r} \right| \psi_{i,f} \rangle = \left\langle \mathbf{r} \right| \mathbf{k}_{i,f} \rangle = \frac{1}{(2\pi)^{3/2}} e^{i \mathbf{k}_{i,f} \cdot \mathbf{r}}$$

$$\hat{V} = \frac{1}{4\pi\varepsilon_0} \left(\sum_k \frac{-Ze^2}{|\mathbf{r} - \mathbf{a}_k|} + \sum_j \frac{e^2}{|\mathbf{r} - \mathbf{R}_j|} \right)$$



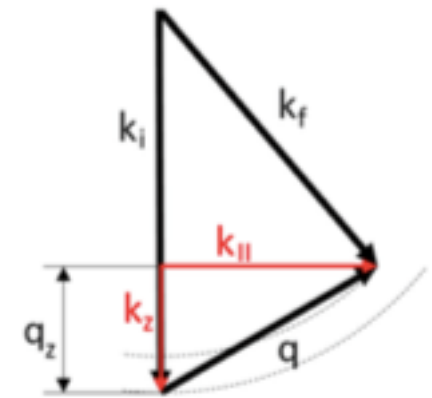
Double differential scattering cross-section

$$W_{i \rightarrow f} = \frac{2\pi}{\hbar} \left| \langle \Psi_f | \hat{V} | \Psi_i \rangle \right|^2 d\nu_f \cdot \delta(E_{|f\rangle} - E_{|i\rangle})$$

$$\langle \Psi_{i,f} \rangle = \langle \psi_{i,f} \rangle \otimes \langle i,f \rangle \quad \langle \mathbf{r} | \psi_{i,f} \rangle = \langle \mathbf{r} | \mathbf{k}_{i,f} \rangle = \frac{1}{(2\pi)^{3/2}} e^{i \mathbf{k}_{i,f} \cdot \mathbf{r}}$$

$$\hat{V} = \frac{1}{4\pi\epsilon_0} \left(\sum_k \frac{-Ze^2}{|\mathbf{r} - \mathbf{a}_k|} + \sum_j \frac{e^2}{|\mathbf{r} - \mathbf{R}_j|} \right)$$

$$\int e^{-i\mathbf{k}_f \cdot \mathbf{r}} \frac{1}{|\mathbf{r} - \mathbf{R}_j|} e^{i\mathbf{k}_i \cdot \mathbf{r}} d^3r = \frac{4\pi}{Q^2} e^{i\mathbf{Q} \cdot \mathbf{R}_j}, \mathbf{Q} = \mathbf{k}_i - \mathbf{k}_f$$



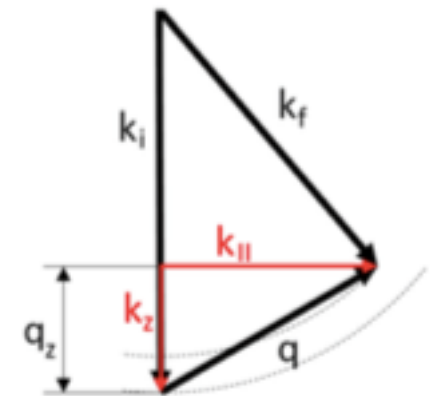
Double differential scattering cross-section

$$W_{i \rightarrow f} = \frac{2\pi}{\hbar} \left| \left\langle \Psi_f \right| \hat{V} \left| \Psi_i \right\rangle \right|^2 d\nu_f \cdot \delta(E_{|f\rangle} - E_{|i\rangle})$$

$$\left| \Psi_{i,f} \right\rangle = \left| \psi_{i,f} \right\rangle \otimes \left| i,f \right\rangle \quad \left\langle \mathbf{r} \right| \psi_{i,f} \rangle = \left\langle \mathbf{r} \right| \mathbf{k}_{i,f} \rangle = \frac{1}{(2\pi)^{3/2}} e^{i \mathbf{k}_{i,f} \cdot \mathbf{r}}$$

$$\hat{V} = \frac{1}{4\pi\epsilon_0} \left(\sum_k \frac{-Ze^2}{|\mathbf{r} - \mathbf{a}_k|} + \sum_j \frac{e^2}{|\mathbf{r} - \mathbf{R}_j|} \right)$$

$$\int e^{-i \mathbf{k}_f \cdot \mathbf{r}} \frac{1}{|\mathbf{r} - \mathbf{R}_j|} e^{i \mathbf{k}_i \cdot \mathbf{r}} d^3 r = \frac{4\pi}{Q^2} e^{i \mathbf{Q} \cdot \mathbf{R}_j}, \mathbf{Q} = \mathbf{k}_i - \mathbf{k}_f$$

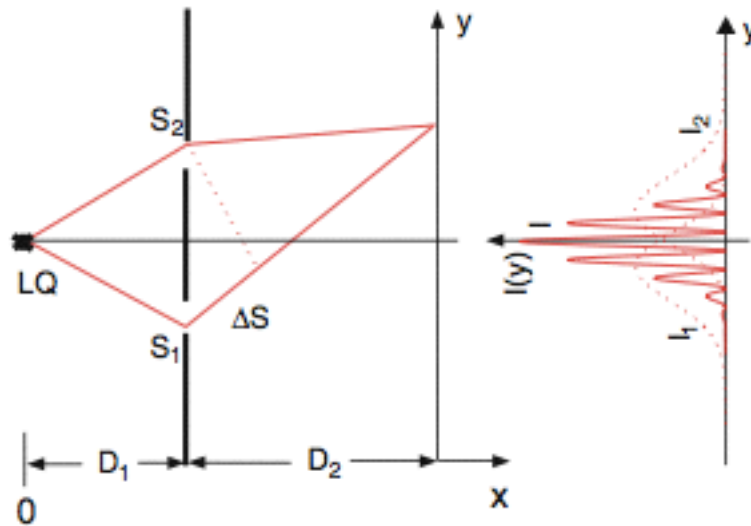


$$\frac{\partial^2 \sigma}{\partial E \partial \Omega} = \frac{4\gamma^2}{a_0^2} \frac{k_f}{k_i} \frac{1}{Q^4} \underbrace{\sum_i \sum_f \sum_j \left| \left\langle f \right| e^{i \mathbf{Q} \cdot \mathbf{R}_j} \left| i \right\rangle \right|^2 \cdot \delta(E_{|f\rangle} - E_{|i\rangle} - E)}_{S(\mathbf{Q}, E)}$$

Dynamic form factor (DFF)



Interferometric EELS (the mixed DFF)

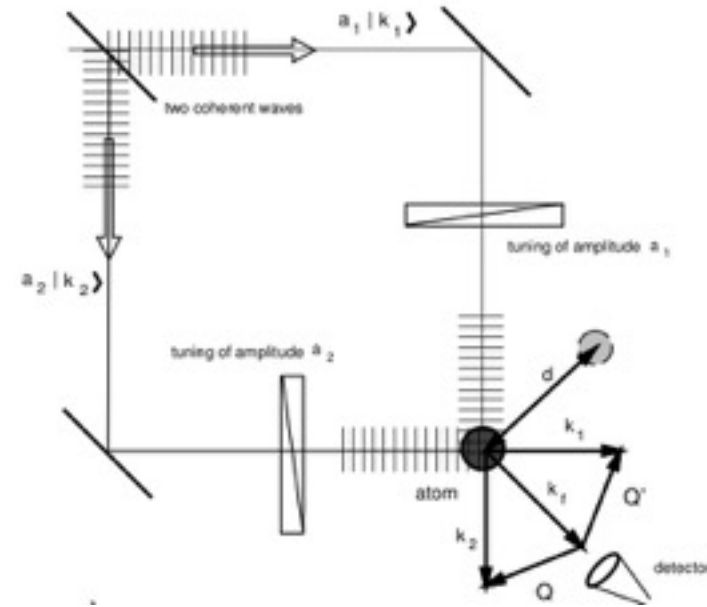
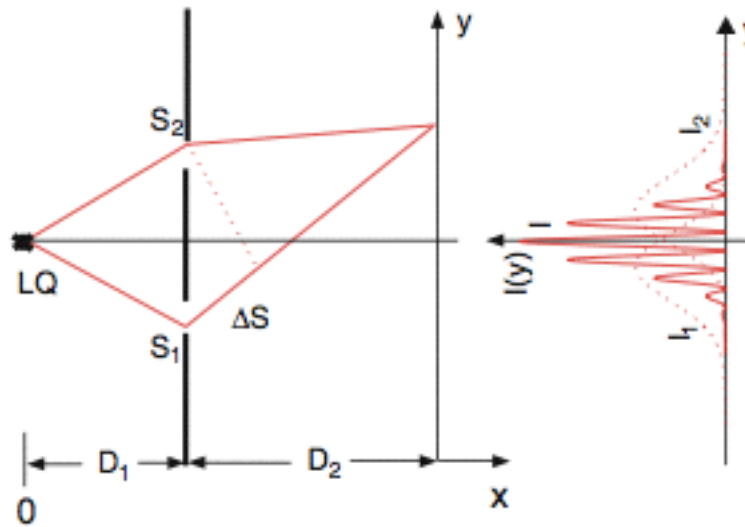


$$I \propto A_1^2 + A_2^2 + 2\Re \left[A_1 A_2^* \cdot e^{i(\varphi_1 - \varphi_2)} \right]$$

Demtröder, Experimentalphysik 3, Springer 2010



Interferometric EELS (the mixed DFF)



$$I \propto A_1^2 + A_2^2 + 2\Re \left[A_1 A_2^* \cdot e^{i(\varphi_1 - \varphi_2)} \right]$$

$$|\psi_i\rangle = a_1 |\mathbf{k}_1\rangle + a_2 |\mathbf{k}_2\rangle$$

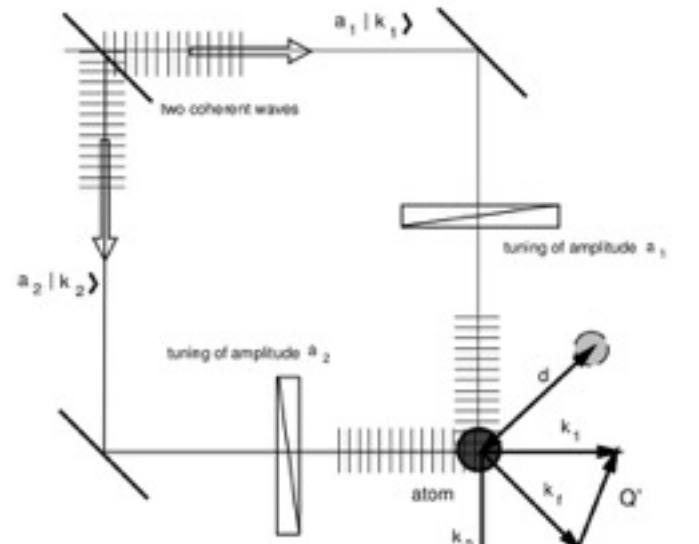
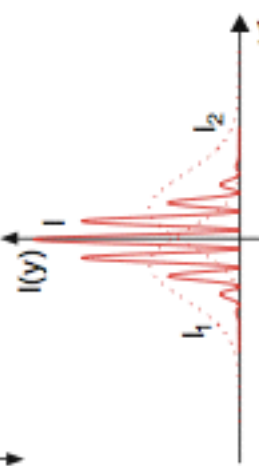
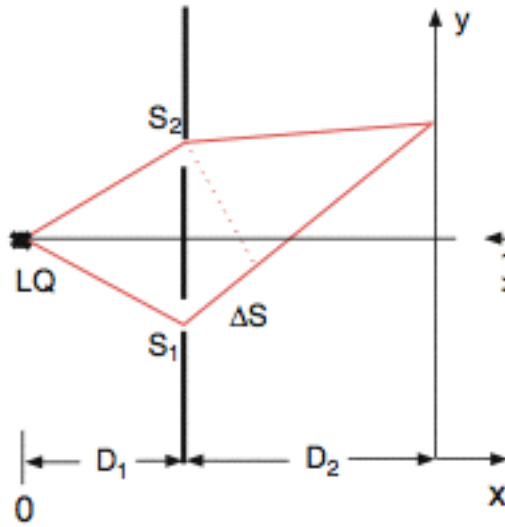
Demtröder, Experimentalphysik 3, Springer 2010

Kohl & Rose, 1985

Nelhiebel, PhD thesis, 1999



Interferometric EELS (the mixed DFF)



$$I \propto A_1^2 + A_2^2 + 2\Re \left[A_1 A_2^* \cdot e^{i(\varphi_1 - \varphi_2)} \right]$$

$$|\psi_i\rangle = a_1 |\mathbf{k}_1\rangle + a_2 |\mathbf{k}_2\rangle$$

$$\frac{\partial^2 \sigma}{\partial E \partial \Omega} = \frac{4\gamma^2}{a_0^2} \frac{k_f}{k_0} \left[\left| a_1 \right|^2 \frac{1}{Q^4} S(\mathbf{Q}, E) + \left| a_2 \right|^2 \frac{1}{Q'^4} S(\mathbf{Q}', E) + 2\Re \left[a_1 a_2^* \frac{1}{Q^2 Q'^2} S(\mathbf{Q}, \mathbf{Q}', E) \right] \right]$$

$$S(\mathbf{Q}, \mathbf{Q}', E) = \sum_i \sum_f \sum_j \langle f | e^{i\mathbf{Q} \cdot \mathbf{R}_j} | i \rangle \sum_{j'} \langle i | e^{-i\mathbf{Q}' \cdot \mathbf{R}_{j'}} | f \rangle \cdot \delta(E_{|f\rangle} - E_{|i\rangle} - E)$$

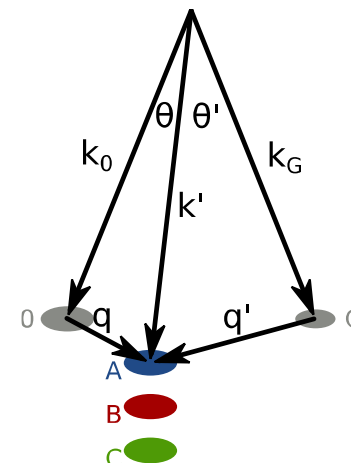
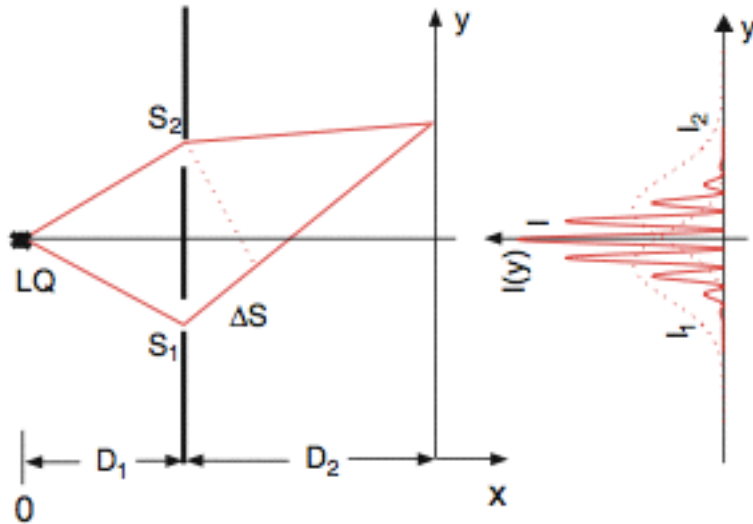
Kohl & Rose, 1985

Demtröder, Experimentalphysik 3, Springer 2010

Nelhiebel, PhD thesis, 1999



Interferometric EELS (the mixed DFF)



$$I \propto A_1^2 + A_2^2 + 2\Re \left[A_1 A_2^* \cdot e^{i(\varphi_1 - \varphi_2)} \right]$$

$$|\psi_i\rangle = a_1 |\mathbf{k}_1\rangle + a_2 |\mathbf{k}_2\rangle$$

$$\frac{\partial^2 \sigma}{\partial E \partial \Omega} = \frac{4\gamma^2}{a_0^2} \frac{k_f}{k_0} \left[\left| a_1 \right|^2 \frac{1}{Q^4} S(\mathbf{Q}, E) + \left| a_2 \right|^2 \frac{1}{Q'^4} S(\mathbf{Q}', E) + 2\Re \left[a_1 a_2^* \frac{1}{Q^2 Q'^2} S(\mathbf{Q}, \mathbf{Q}', E) \right] \right]$$

$$S(\mathbf{Q}, \mathbf{Q}', E) = \sum_i \sum_f \sum_j \langle f | e^{i\mathbf{Q} \cdot \mathbf{R}_j} | i \rangle \sum_{j'} \langle i | e^{-i\mathbf{Q}' \cdot \mathbf{R}_{j'}} | f \rangle \cdot \delta(E_{|f\rangle} - E_{|i\rangle} - E)$$

Kohl & Rose, 1985

Demtröder, Experimentalphysik 3, Springer 2010

Nelhiebel, PhD thesis, 1999





The MDFF for crystals

$$S(\mathbf{Q}, \mathbf{Q}', E)$$



The MDFF for crystals

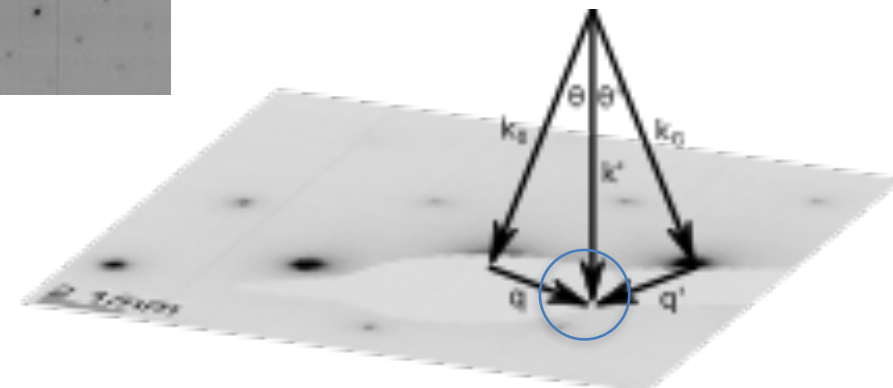
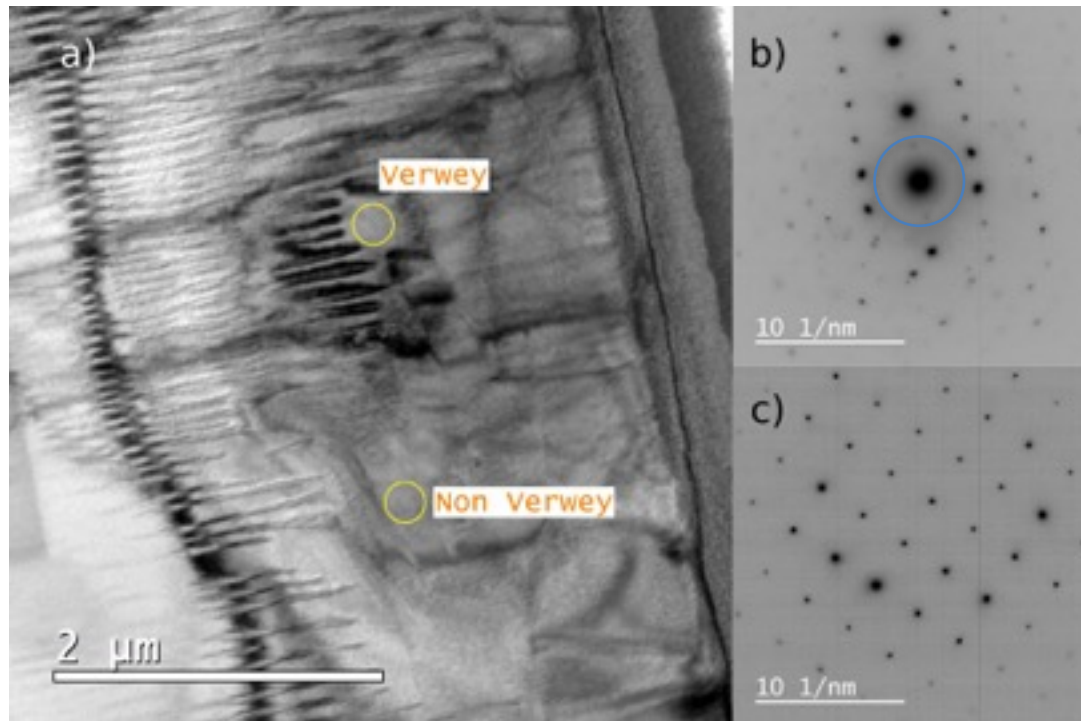
$$S(\mathbf{Q}, \mathbf{Q}', E)$$

$$\left\langle j_\lambda(Q) \right\rangle_{\nu n j LS} = \int_0^\infty u_{\nu LS}(R)^* j_\lambda(QR) u_{njS}(R) R^2 dR$$

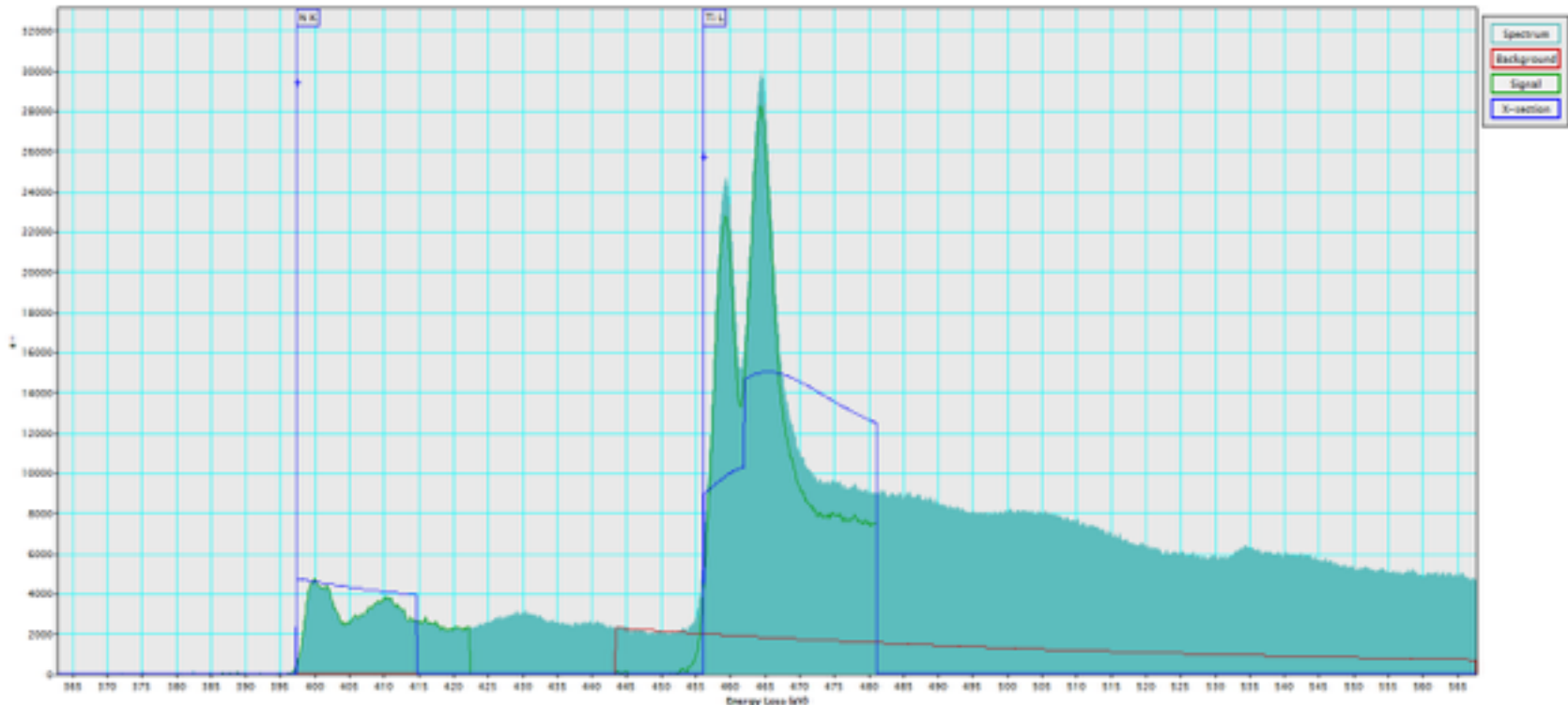
$$X_{LMS, L'M'S'}(E) := \sum_\nu \left(D_{LMS}^\nu \right)^* D_{L'M'S'}^\nu \delta(E - E_\nu)$$



Experimental realisation



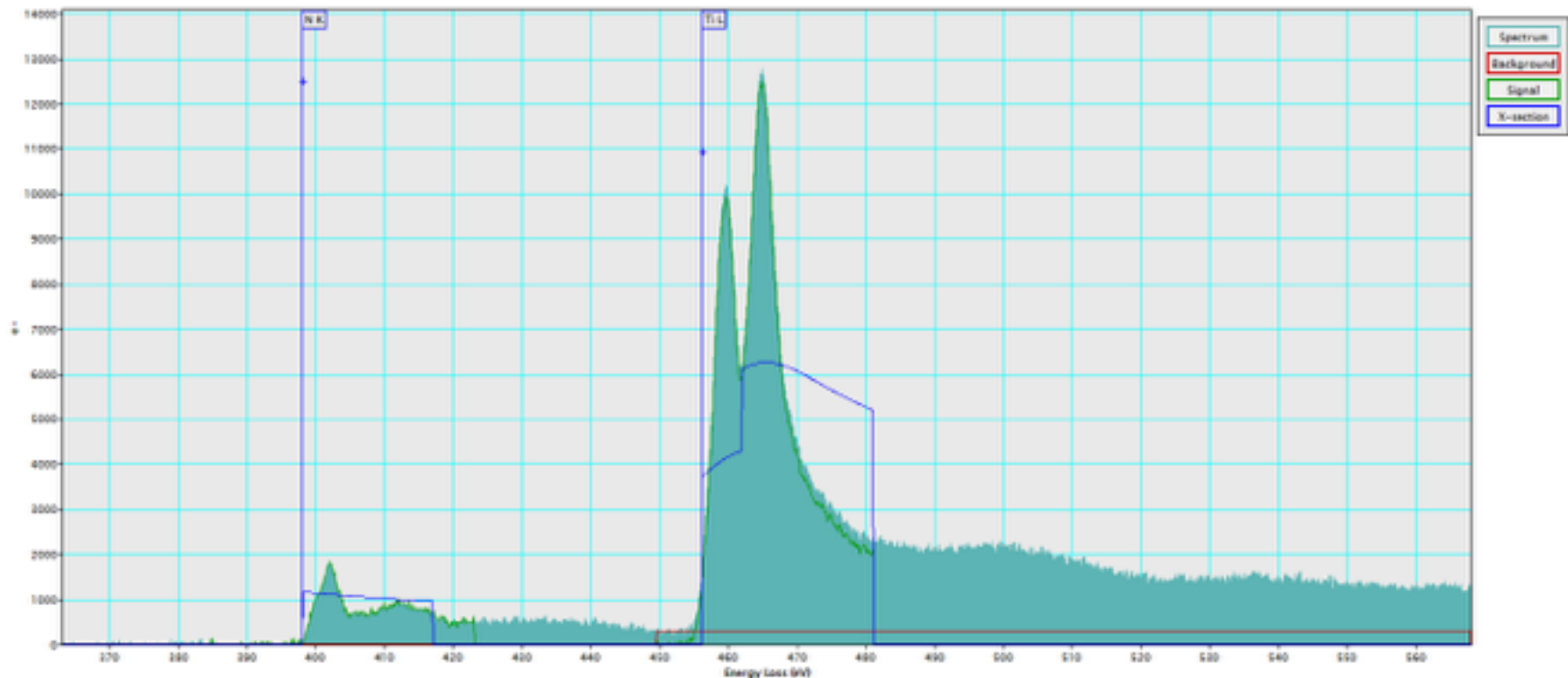
Experimental spectra



Relative quantification:
Elem. Atomic ratio (/Ti) Percent content
N 0.80 ± 0.113 44.34
Ti 1.00 ± 0.000 55.66



Experimental spectra

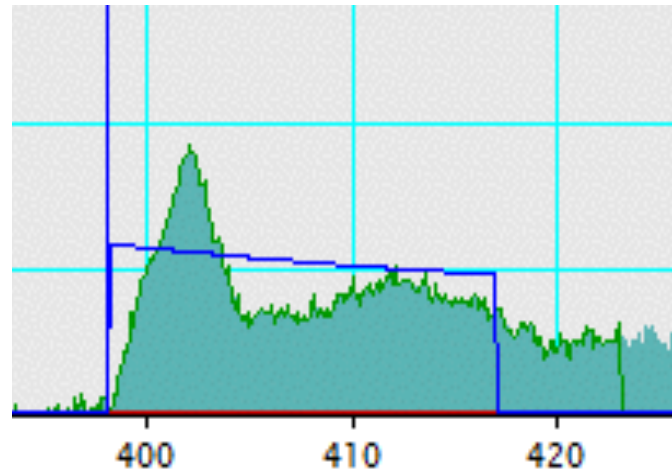
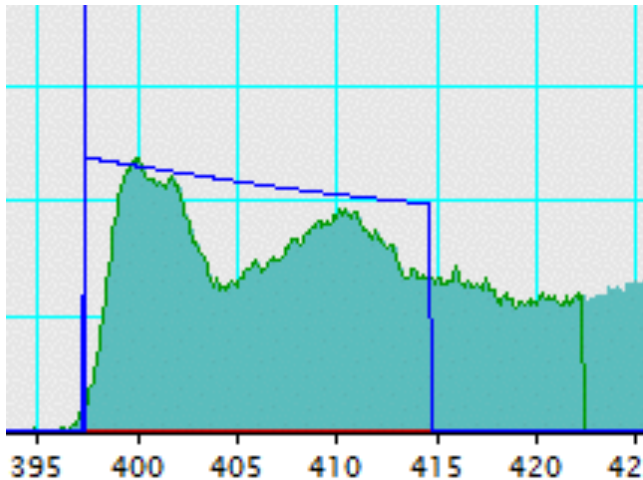


Relative quantification:

	Elem.	Atomic ratio (/Ti)	Percent content
N		0.47 ± 0.067	32.01
Ti		1.00 ± 0.000	67.99



Experimental spectra

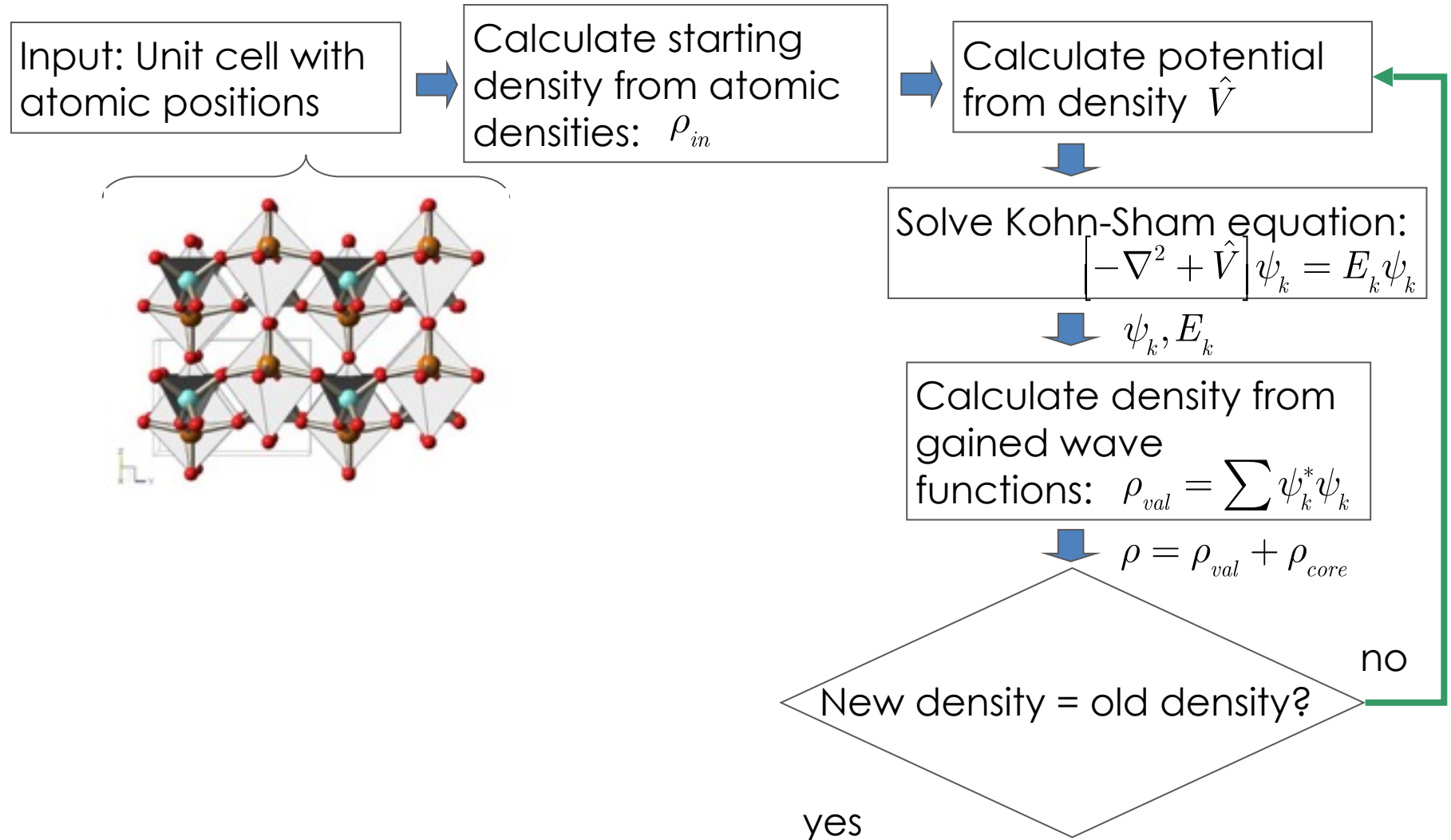


Differences in fine structure: different electronic structure





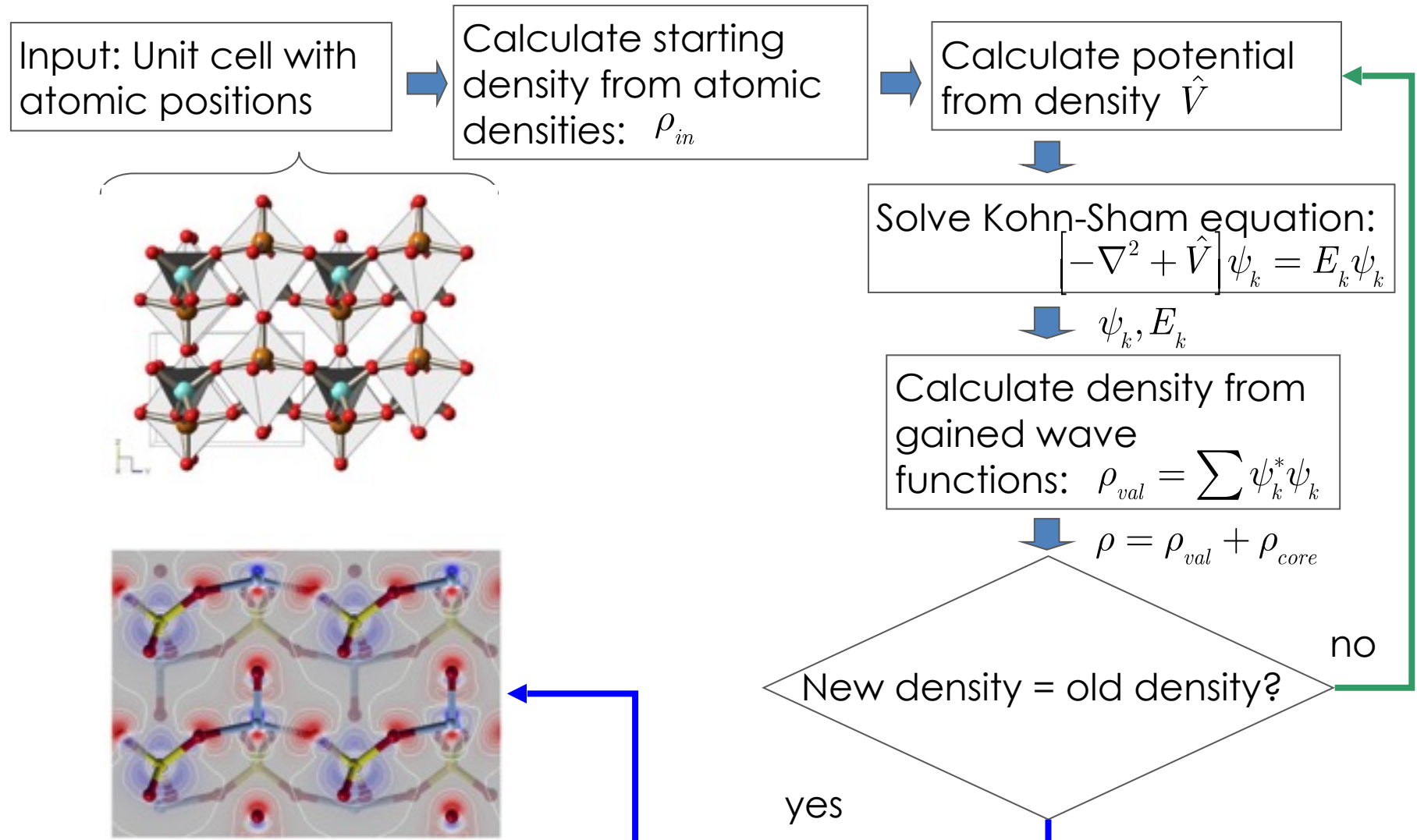
WIEN2k simulation



Payne et al., Rev. Mod. Phys. 64, 1045 (1992)



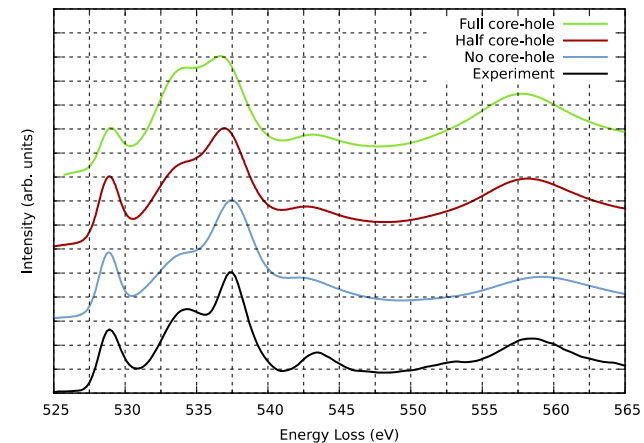
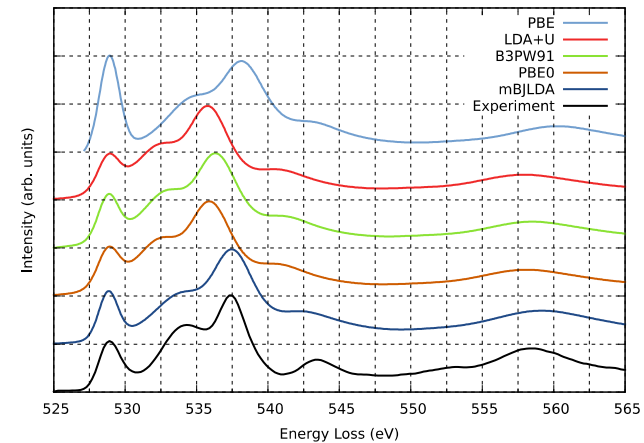
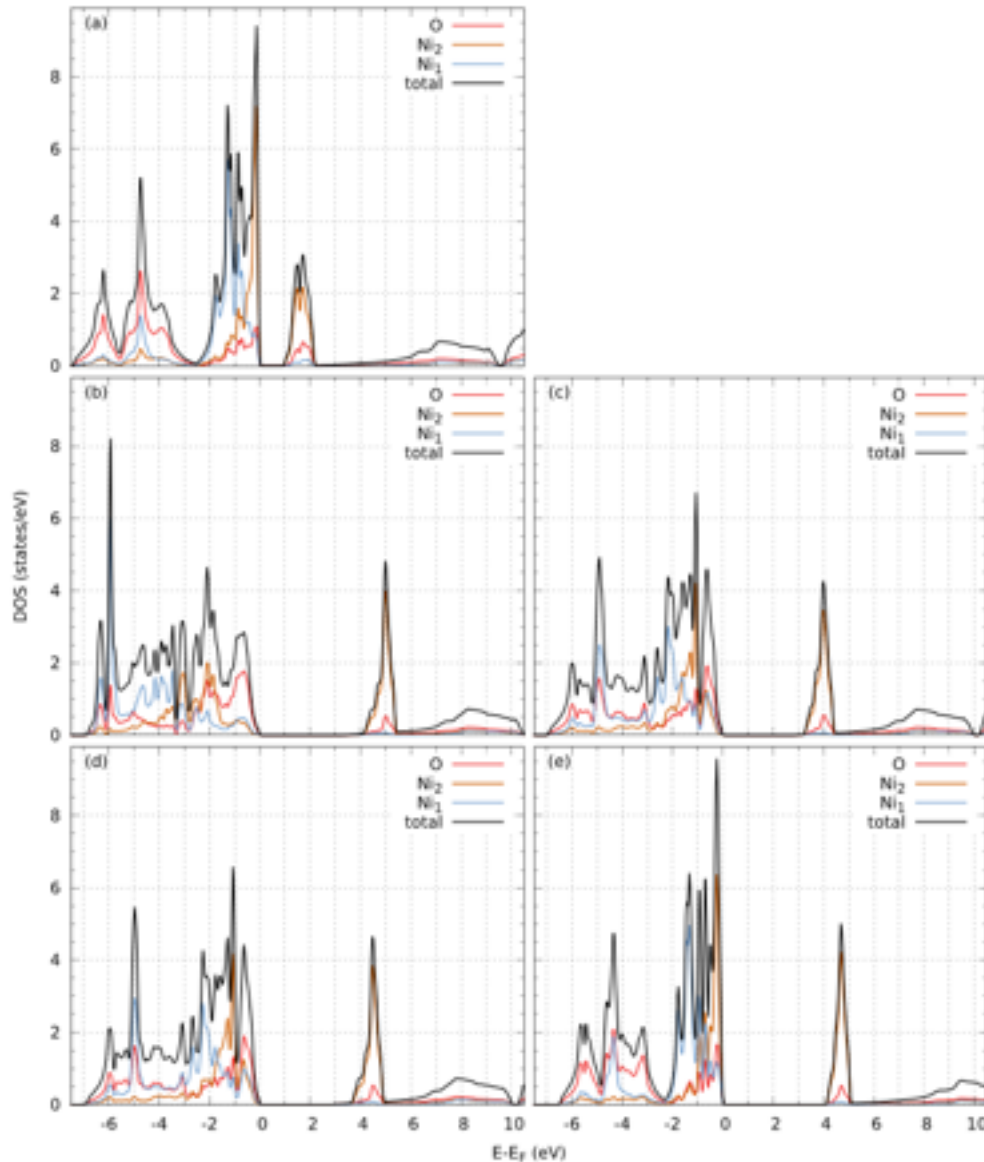
WIEN2k simulation



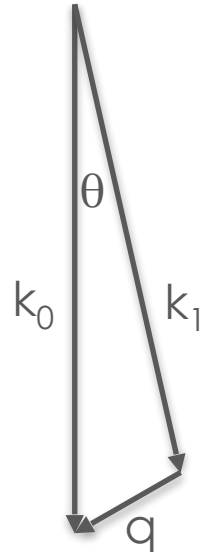
Payne et al., Rev. Mod. Phys. 64, 1045 (1992)



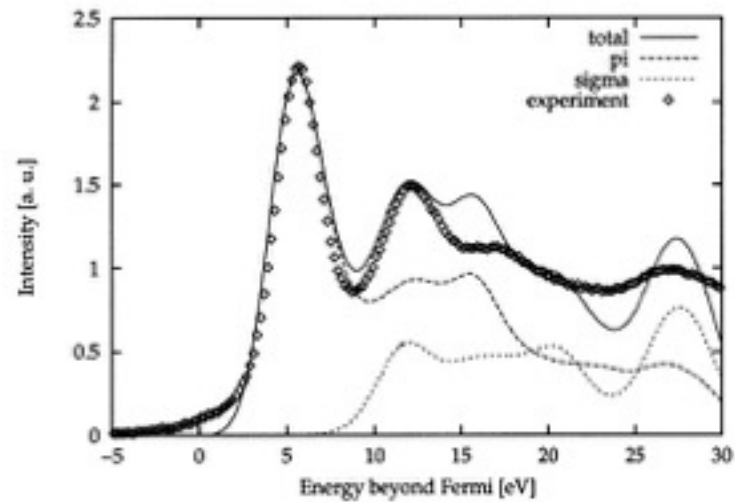
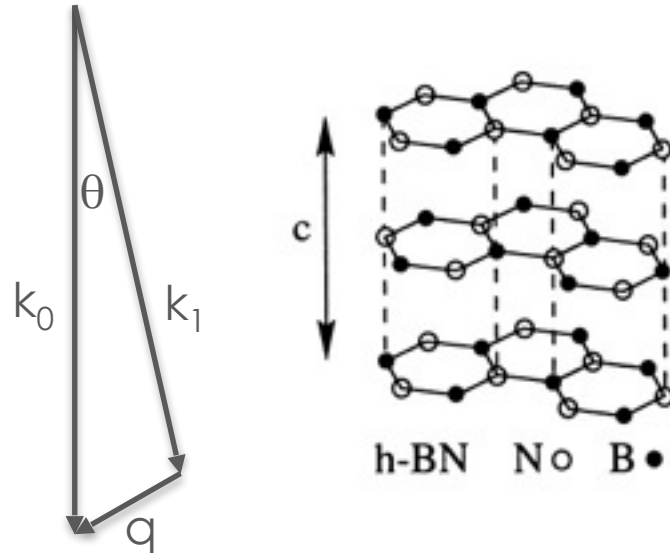
TELNES – calculation of spectra



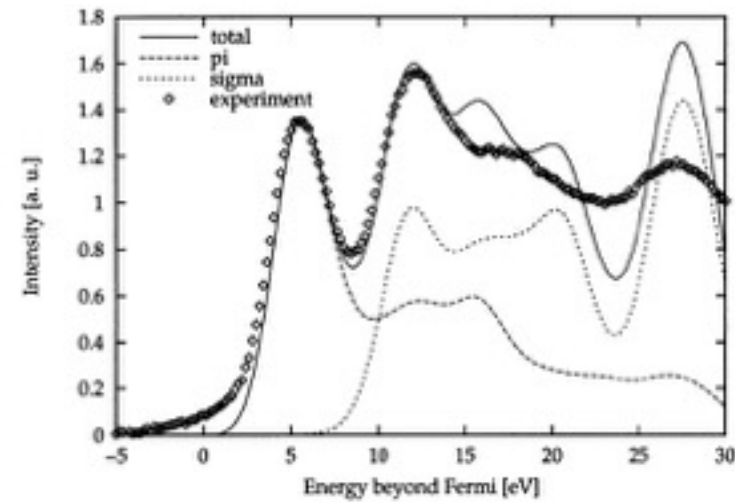
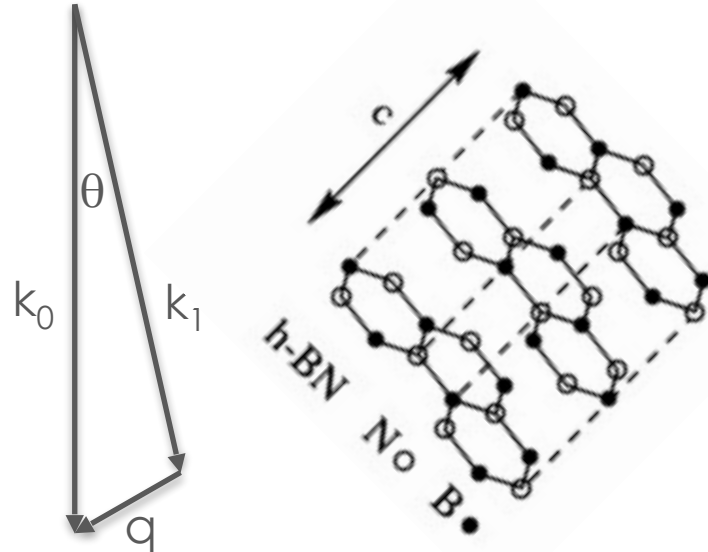
Effects of anisotropy



Effects of anisotropy



Effects of anisotropy

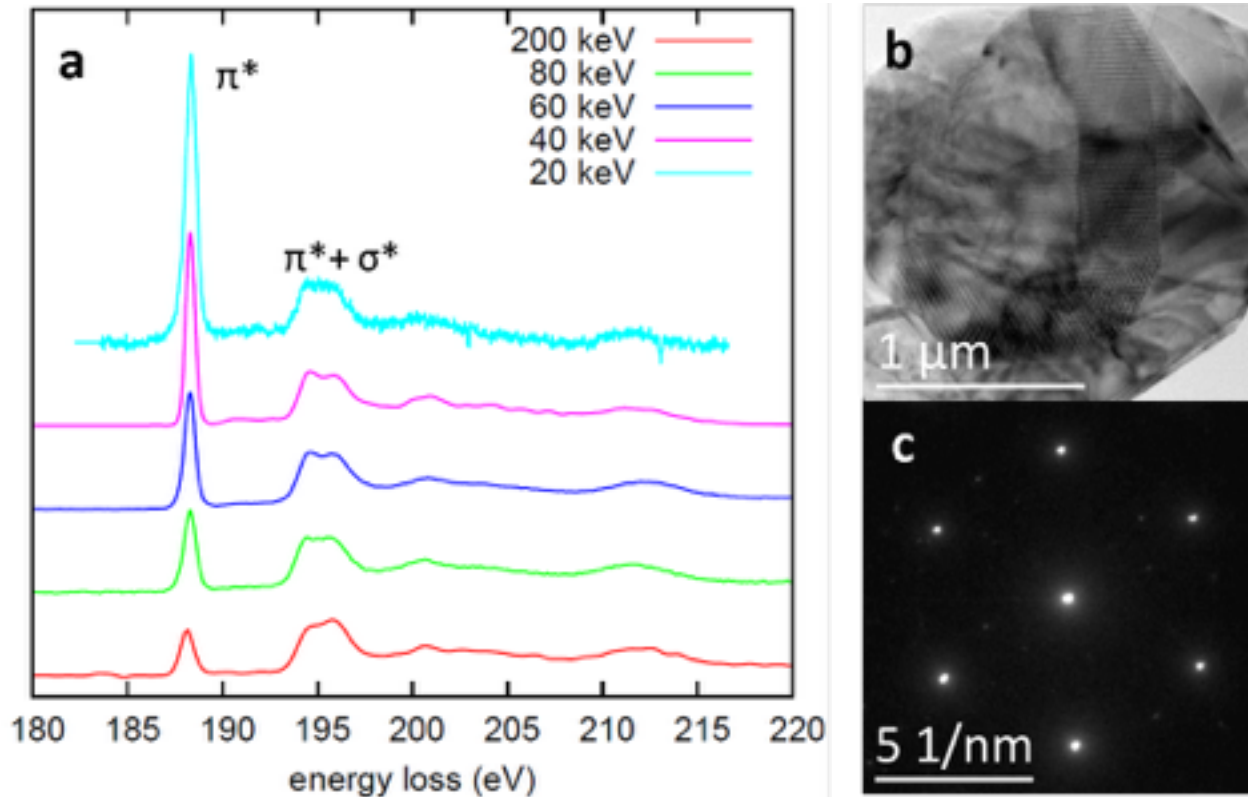


Hébert-Souche et al., UM 83 (2000), 9-16



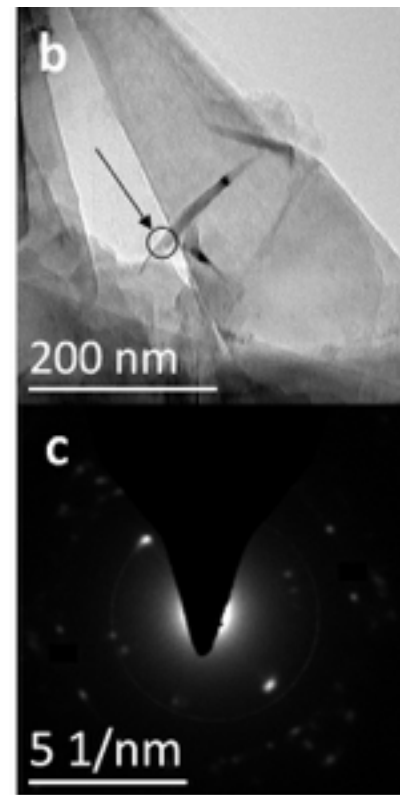
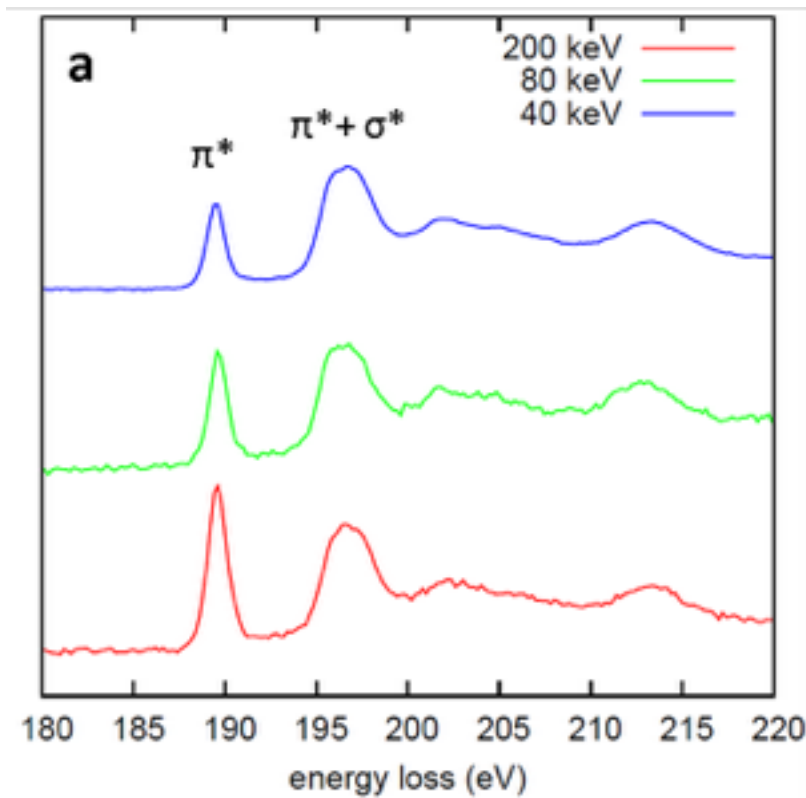
Anisotropy – experiment 1

Orientation: c-axis parallel to electron-beam



Anisotropy – experiment 2

Orientation: c-axis perpendicular to electron-beam



Energy-loss magnetic chiral dichroism

- EMCD, 2006
- Polarisation vector



momentum transfer vector

$$\varepsilon + i \varepsilon'$$

$$q + i q'$$

Energy-loss magnetic chiral dichroism

- EMCD, 2006
- Polarisation vector

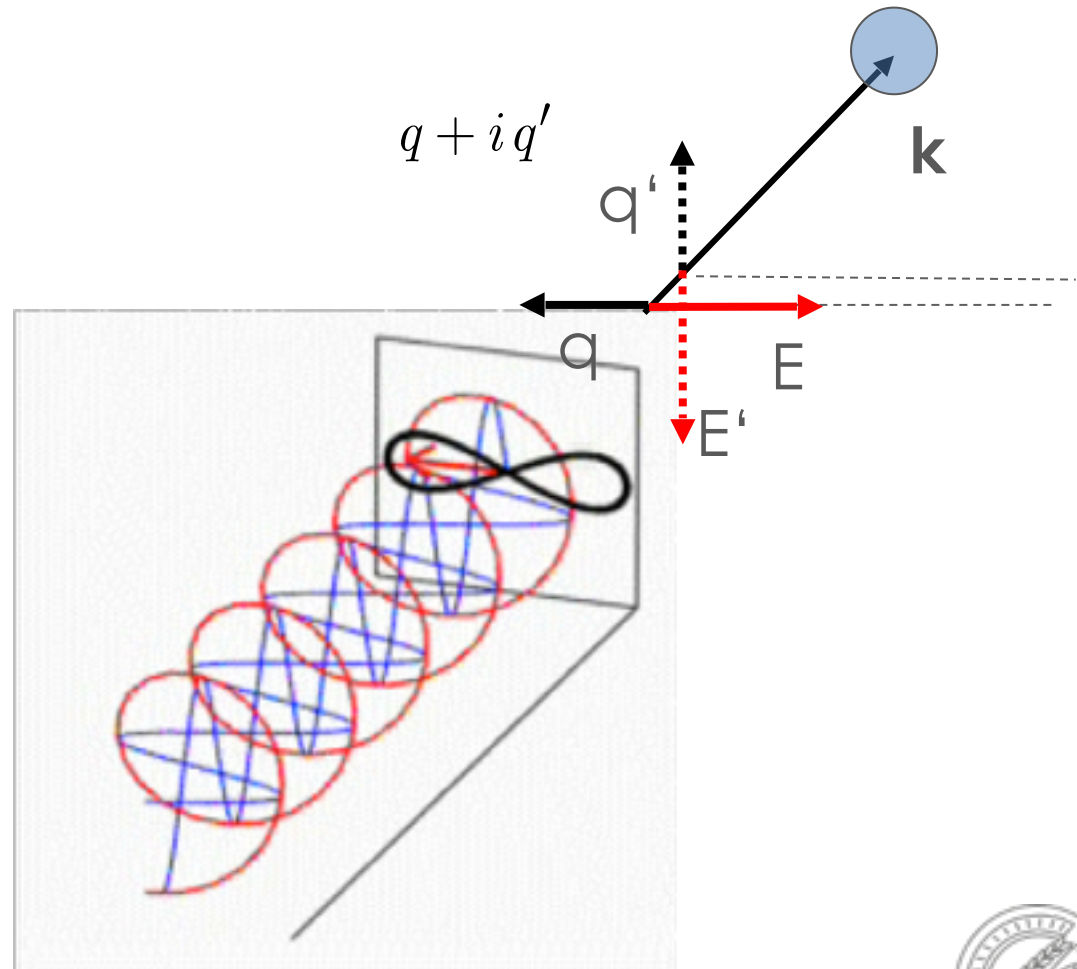


momentum transfer vector

$$\varepsilon + i \varepsilon'$$

$$q + i q'$$

$$\mathbf{k}$$



Energy-loss magnetic chiral dichroism

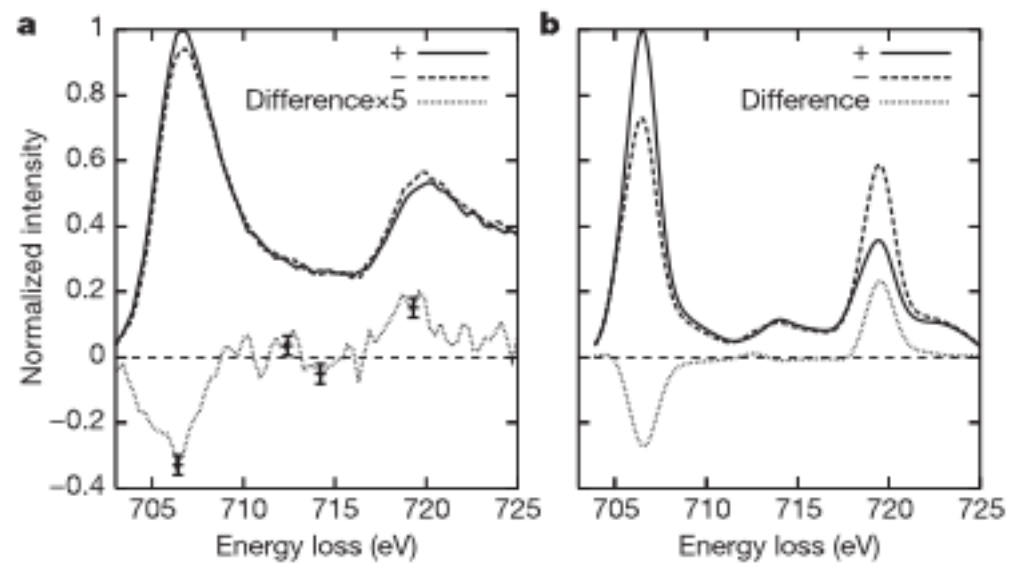
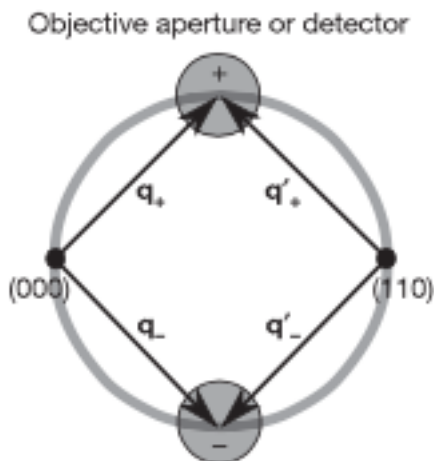
- EMCD, 2006
- Polarisation vector



momentum transfer vector

$$\varepsilon + i \varepsilon'$$

$$q + i q'$$



Energy-loss magnetic chiral dichroism

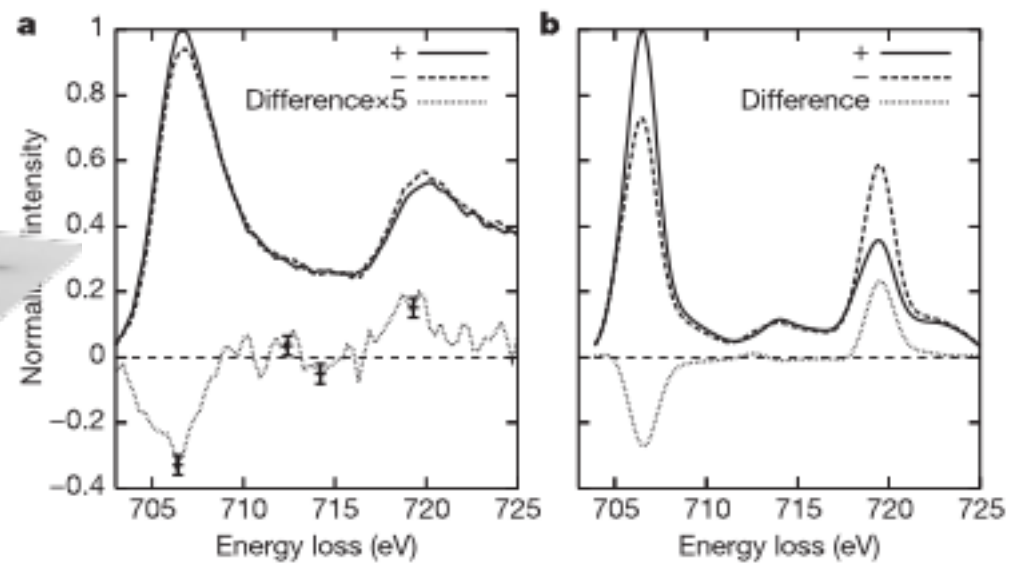
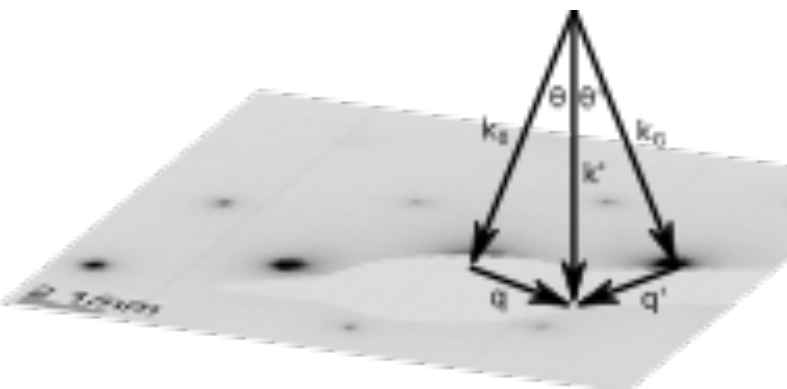
- EMCD, 2006
- Polarisation vector



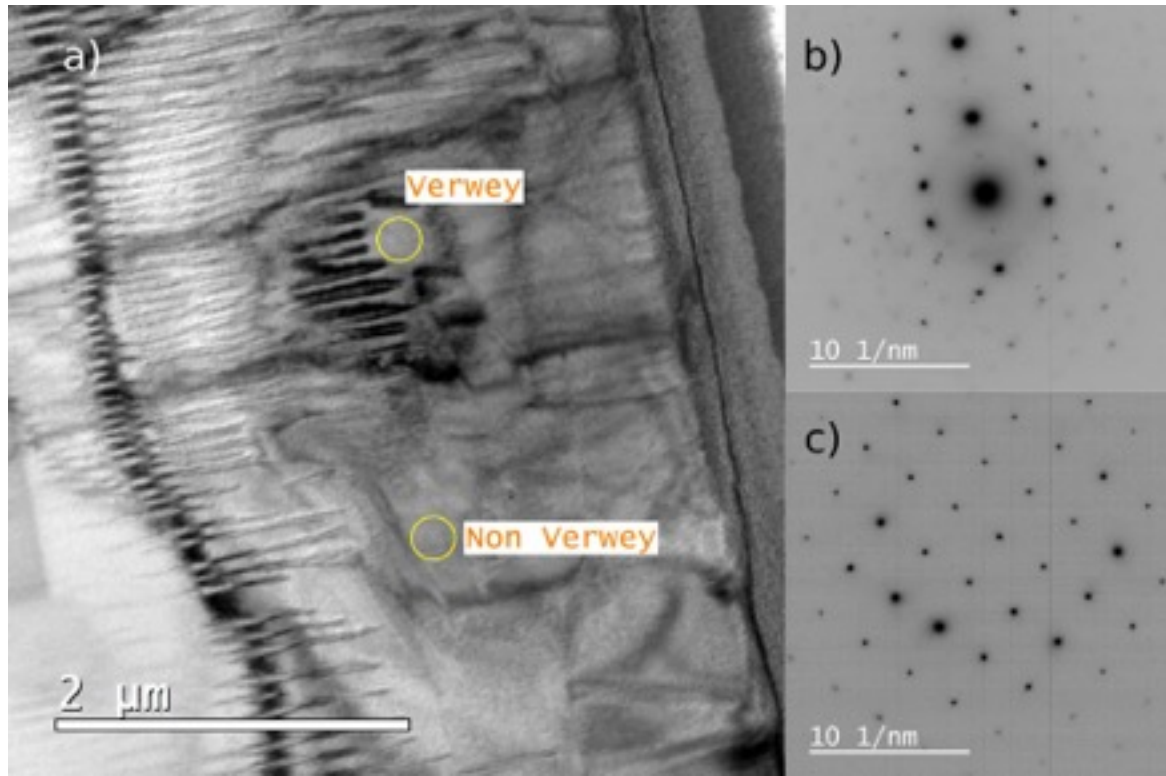
momentum transfer vector

$$\varepsilon + i \varepsilon'$$

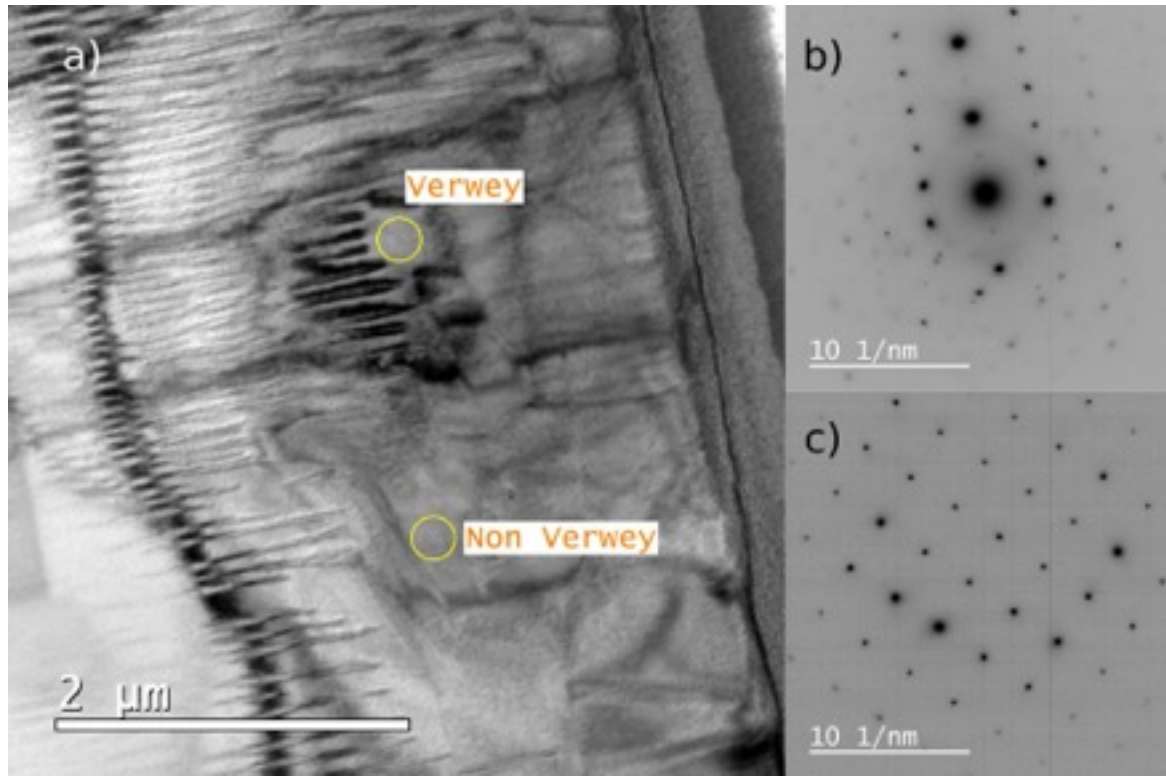
$$q + i q'$$



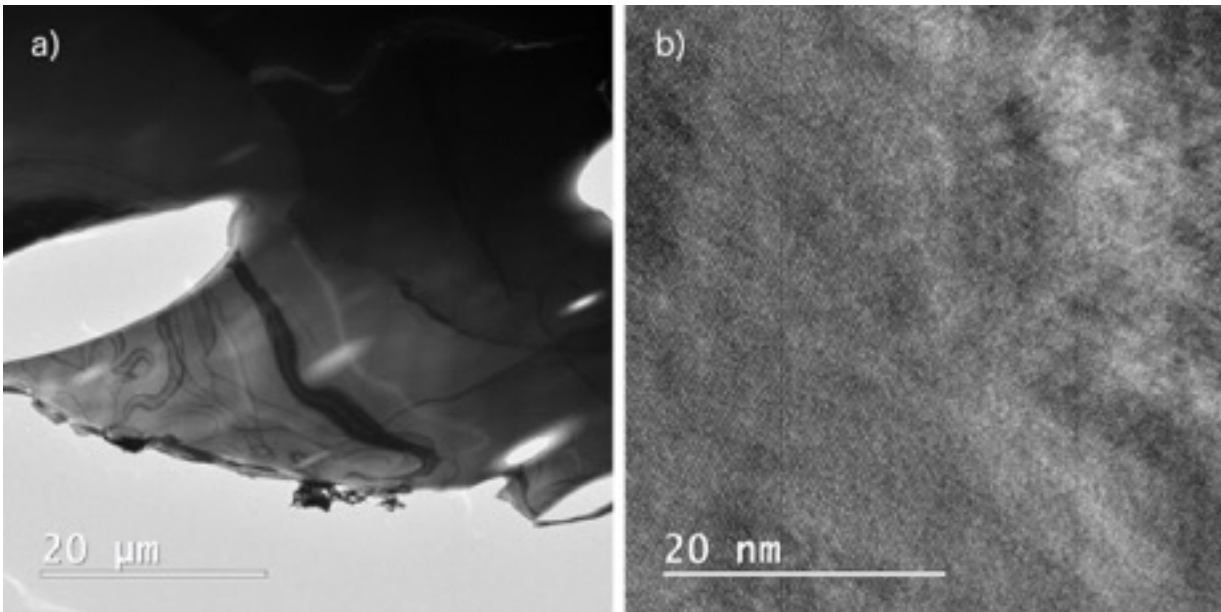
EMCD – example 1



EMCD – example 1

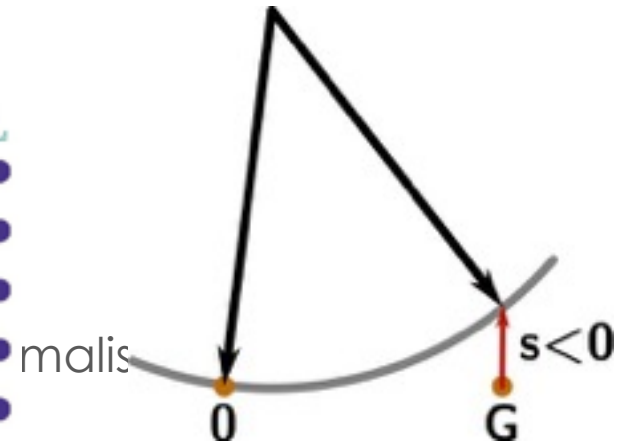
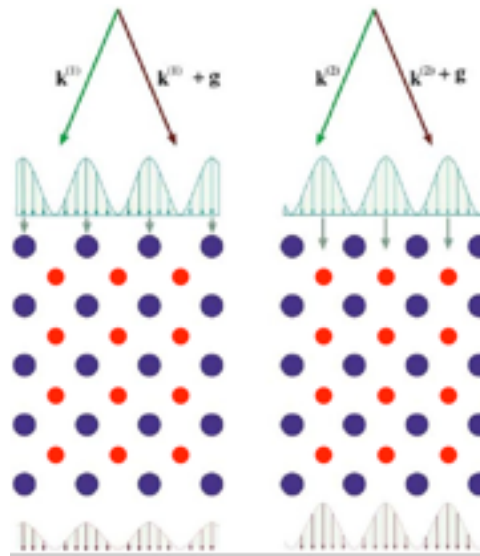
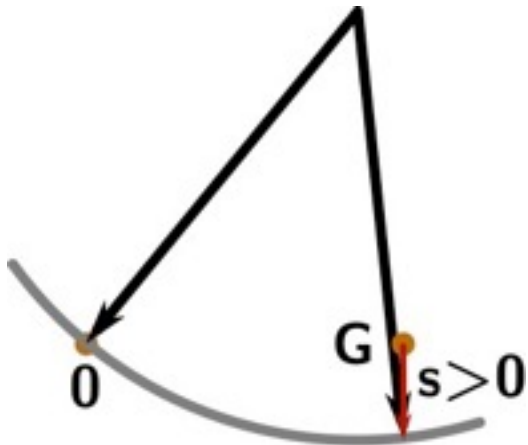


EMCD – example 2



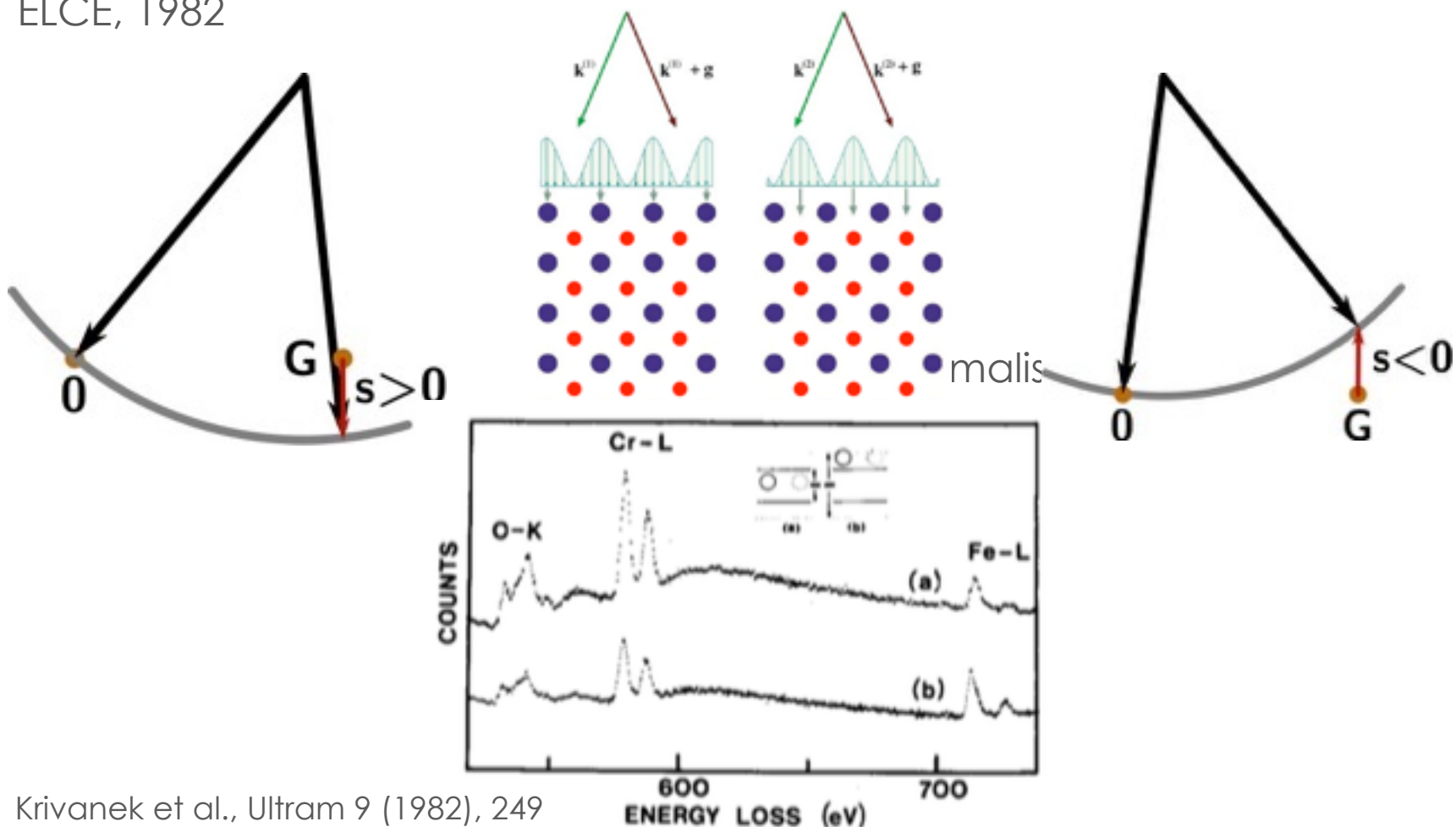
Energy losses by channelled electrons

ELCE, 1982



Energy losses by channelled electrons

ELCE, 1982



Krivanek et al., Ultram 9 (1982), 249

Fig. 7. EEL spectra from chromite. (a) Octahedral sites selected.
(b) Tetrahedral sites selected.



ELCE simulations

Incoming wave, scattering, outgoing wave
Input: crystal, exp. parameters, scattering model
Output: Bloch waves, intensity maps, thickness dependence

Löffler & Schattschneider, Ultram 110 (2010), 831

Hetaba, Diploma-Thesis, 2011

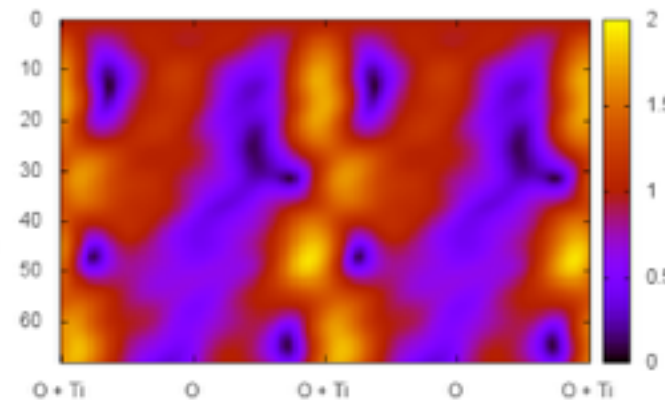
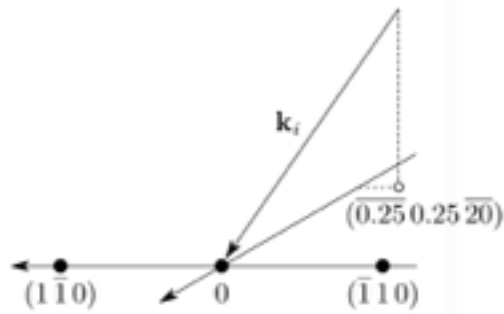
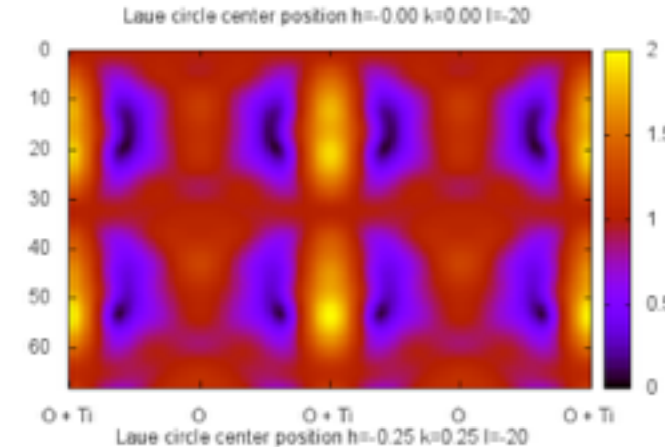
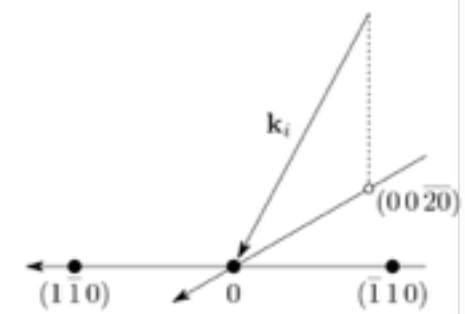


ELCE simulations

Incoming wave, scattering, outgoing wave

Input: crystal, exp. parameters, scattering model

Output: Bloch waves, intensity maps, thickness dependence



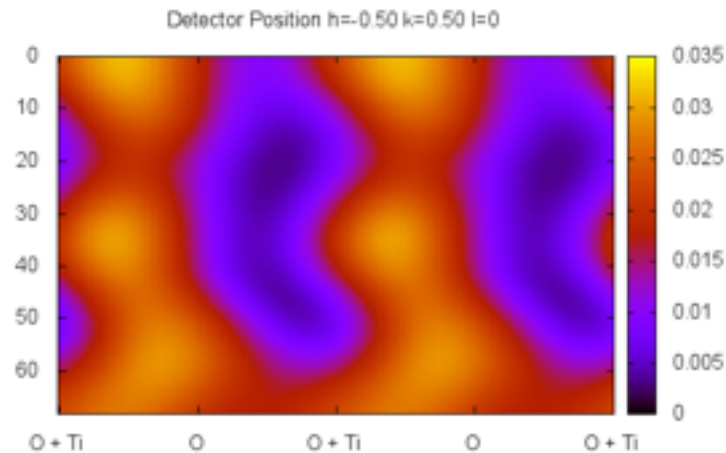
Löffler & Schattschneider, Ultram 110 (2010), 831

Hetaba, Diploma-Thesis, 2011



ELCE simulations

Incoming wave, scattering, outgoing wave
Input: crystal, exp. parameters, scattering model
Output: Bloch waves, intensity maps, thickness dependence



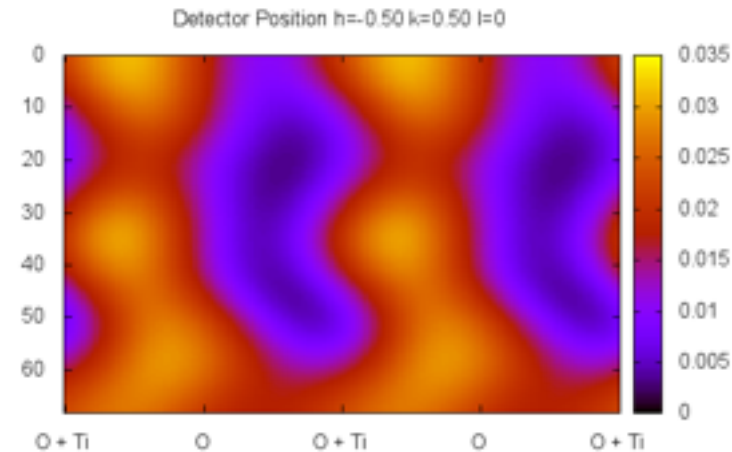
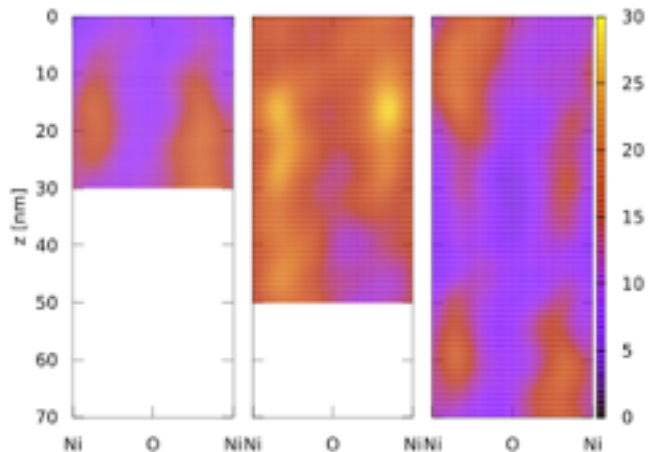
Löffler & Schattschneider, Ultram 110 (2010), 831

Hetaba, Diploma-Thesis, 2011



ELCE simulations

Incoming wave, scattering, outgoing wave
Input: crystal, exp. parameters, scattering model
Output: Bloch waves, intensity maps, thickness dependence



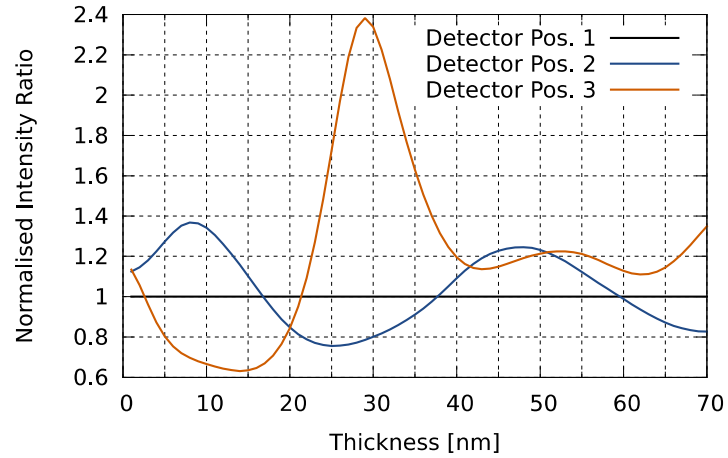
Löffler & Schattschneider, Ultram 110 (2010), 831

Hetaba, Diploma-Thesis, 2011



ELCE simulations

Incoming wave, scattering, outgoing wave
Input: crystal, exp. parameters, scattering model
Output: Bloch waves, intensity maps, thickness dependence

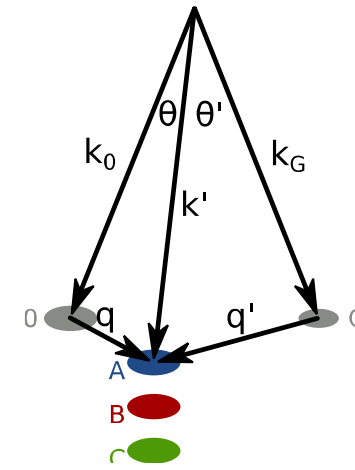
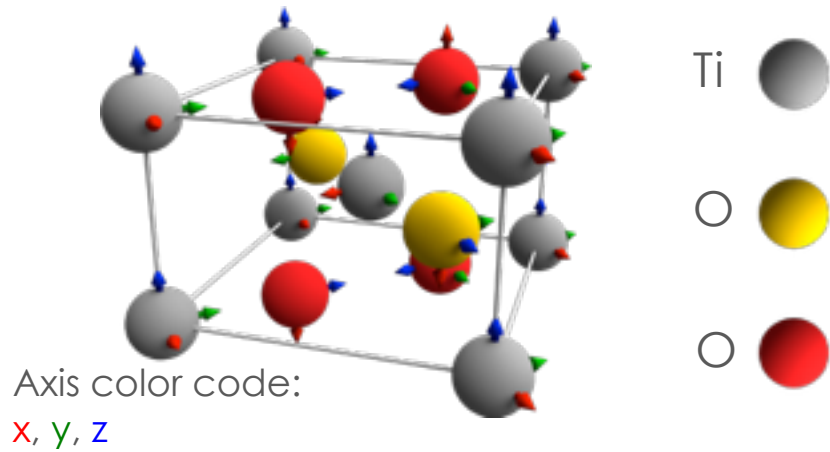


Löffler & Schattschneider, Ultram 110 (2010), 831

Hetaba, Diploma-Thesis, 2011



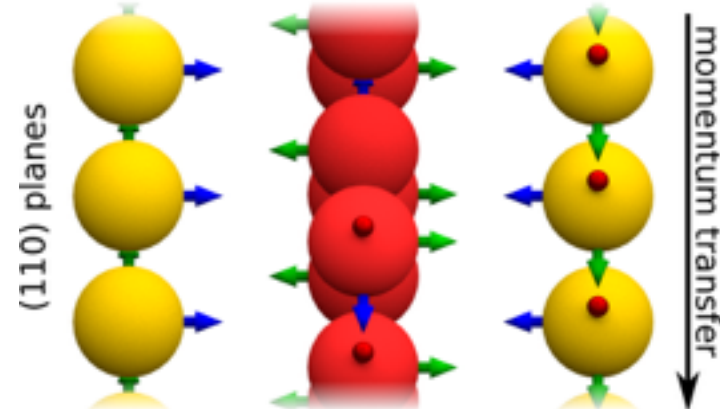
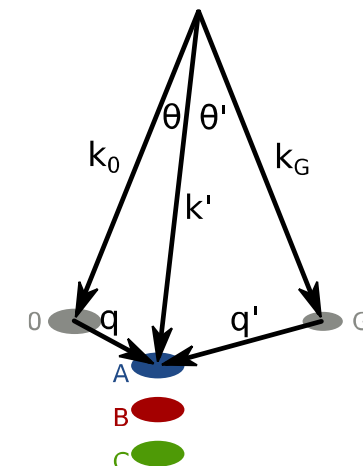
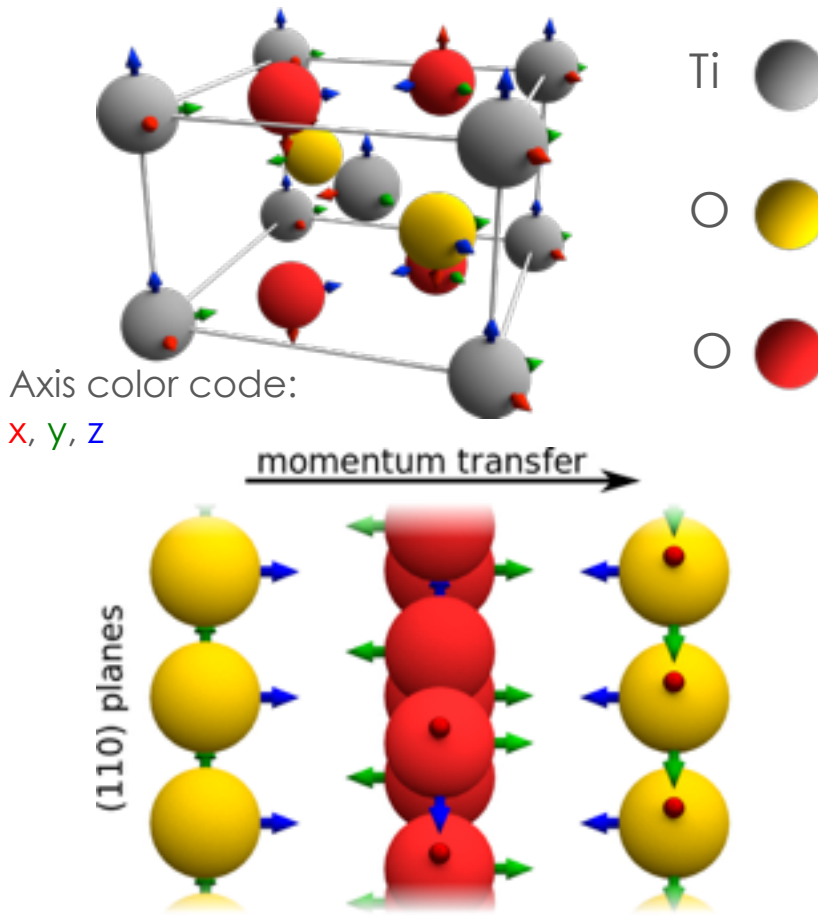
ELCE experiments & simulations



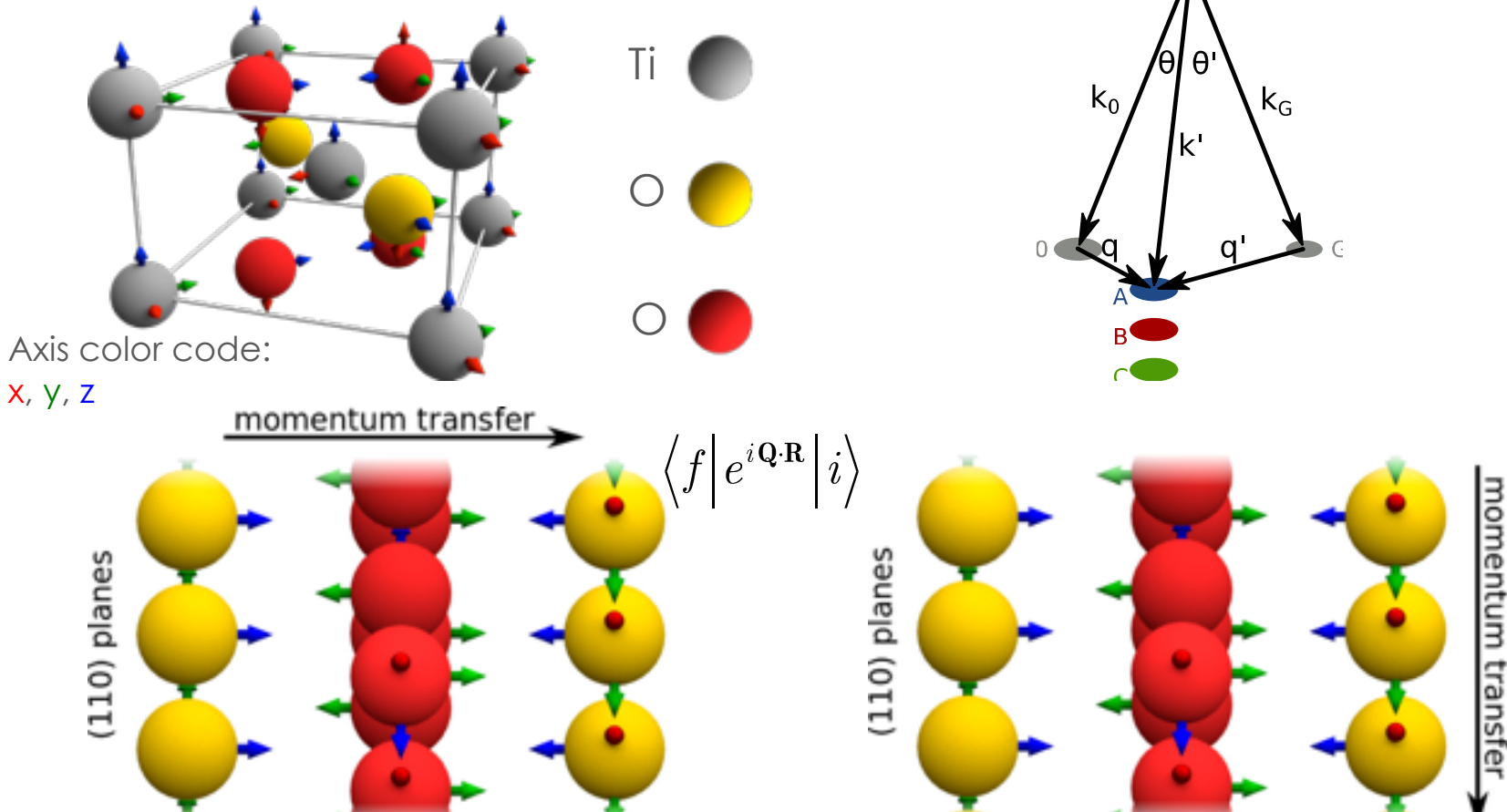
Hetaba, Micron 63 (2014), 15



ELCE experiments & simulations



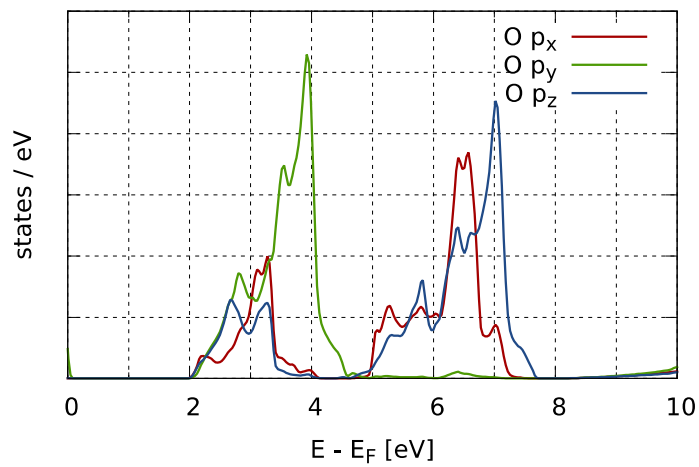
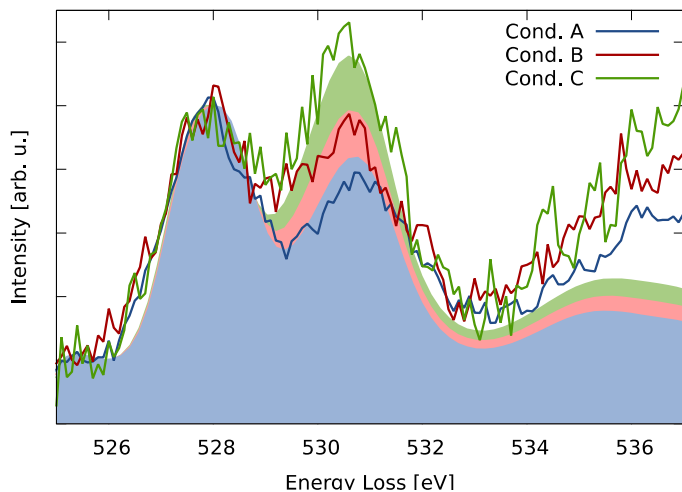
ELCE experiments & simulations



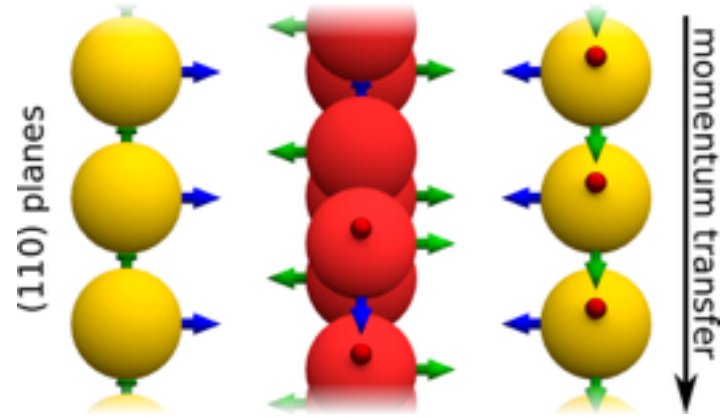
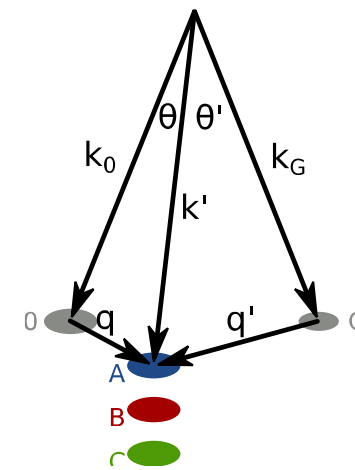
Hetaba, Micron 63 (2014), 15



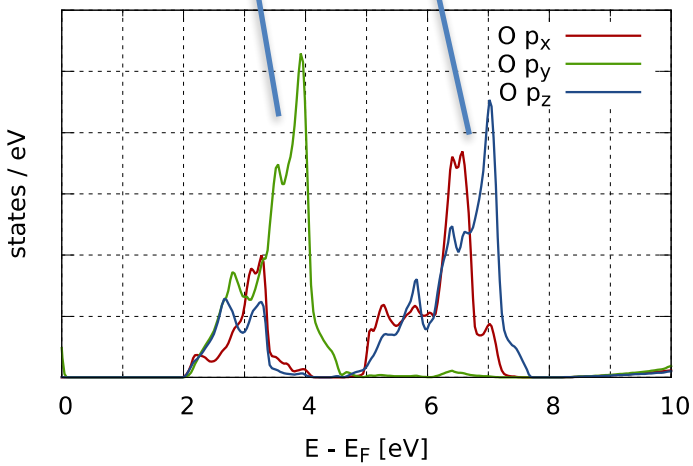
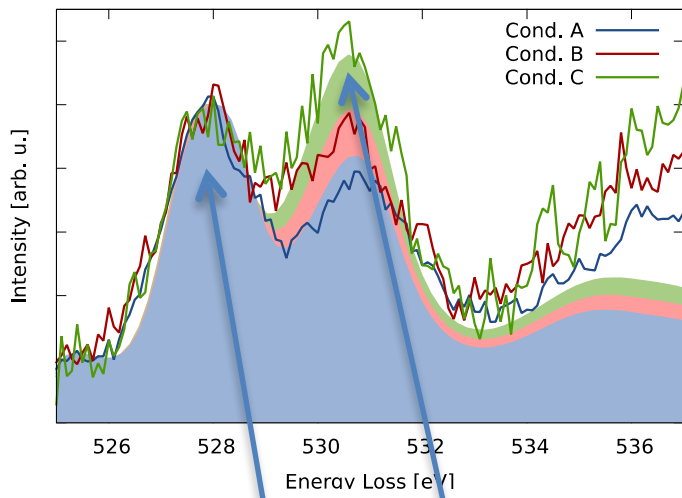
ELCE experiments & simulations



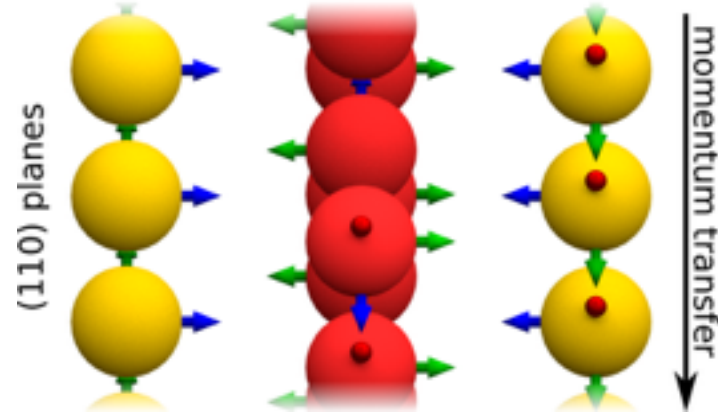
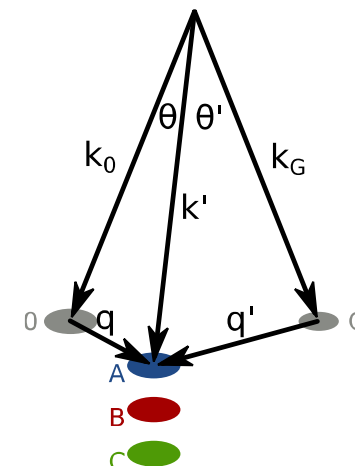
Hetaba, Micron 63 (2014), 15



ELCE experiments & simulations



Hetaba, Micron 63 (2014), 15



Summary

- EELS comparable to XAS
- Available at lower costs
- Almost all TEMs have EELS-capability
- Usually less energy-resolution but higher spatial resolution
- EELS is a versatile analytical methods
- Information about:
 - Elemental composition
 - Thickness
 - Electronic structure
 - Optical properties
 - Magnetic properties

